**NTNU – Trondheim**
Norwegian University of
Science and Technology

# Experimental Study of Stress Dependent P-and S-wave Velocities in Both Dry and Saturated Sand

## Kaleem Qadar

Petroleum Geosciences
Submission date:  July 2014
Supervisor:      Rune Martin Holt, IPT

Norwegian University of Science and Technology
Department of Petroleum Engineering and Applied Geophysics

# NTNU
## Norwegian University of Science and Technology

**Experimental Study of Stress Dependent P-and S-wave Velocities in Both Dry and Saturated Sand**

**By: Kaleem Qadar**

**Trondheim, July, 2014**

**Academic supervisor: Rune Martin Holt**

**Department of Petroleum Engineering and Applied Geophysics**

**Norwegian University of Science and Technology**

**Dedication**

Dedicated to My loving parents

# Acknowledgement

First and most I am very grateful to Almighty Allah, who enabled me to complete my master project successfully. A lot of Darood-o-slam to the Holy Prophet (peace be upon him), who is the real source of knowledge, wisdom and guidance.

 I would like to express my extreme gratitude to my supervisor, *Prof Rune Martin Holt*, for his utmost guidance and support throughout my master project. Most Importantly I owe my extremely thankful to my co-supervisor, *Muhammad Hossain bhuiyan*, for his sincere guidance, supervision and help throughout my project work. Who has delivered his valuable suggestions in entire project for completion. Without his suggestions and keen interest, this project wouldn't be possible. In addition I am very thankful to the sintef lab staff and all those who helped me and guide me during my experimental work in lab.

I would also thankful to NTNU who has provided me such a great environment in my entire Master studies.

# Abstract

Vp/Vs ratio is known as lithological and fluid prediction method as well as key part of AVO analysis. This diploma thesis is based on the based on the theoretical and mainly experimental studies to evaluate the behavior of velocities with stress and strain with different stress path. As the physical and chemical behavior of the sediments change with change in overburden stress which has not only influence on the sediments grain structures, sizes, angularity and sorting but it has also a strong influence on elastic and acoustic properties of the rocks. The main idea of the present study was to find that at what extent pore fluid has an effect on the acoustic properties of the sand and sandstone. So for this different experiments has been performed in the laboratory in an oedometer setup with different percentage of brine and also with different grainsized samples both for dry and saturated cases to see the clear effect of fluid on velocities and also the velocities behavior with stress. Data included both the P- and S- wave velocities, strain sensitivity with stress and also porosity change with stress.

In the present study the for case#01 in which Ottawa (OT) sand with different percentage of brine were tested in uniaxial conditions performed in an oedometer setup. The vertical P- and S- wave velocities are found much higher with high concentration of the brine which could possibly because of the sample stiffness which increases with an increase in brine percentage. Moreover the changes in velocities are also found because of an increase in net vertical stress which needs to be considered as well. Similarly the Vp/Vs ratio decreased with in an increase in external stress but at lower stress level it seems to be relatively stable. For the first case stress sensitivity with strain, as all the samples were compacted about 11.0 MPa net vertical stress, so it can be termed as consolidation samples, therefore less strain sensitivity would expected. But the samples with high concentration of brine show high strain sensitivity and viceversa. All the samples show the strain hysteresis because of their inelastic behavior as none of the samples returns to its original shape. Porosity reduction with stress was not found higher so it was more or less stable.

For the second case#02 in which different samples were used with different grain sizes but with same percentage of brine to see the possible fluid effect on velocities and also grain size. But it was clearly observed that P- wave velocity after fluid substitution went higher as compared to the velocities in dry samples. However there is no such change has been found in case of S- wave as it doesn't have any effect with the fluid. In this case velocities were found also stress sensitive as in first case. Similarly there was not such difference has been observed in velocities due to change in grain sizes. While the behavior of, stress strain sensitivity and porosity reduction with stress was found more or less same as in case#01 as discussed above.

# Nomenclature

Vp: P-wave velocity

Vs: S-wave velocity

K: Bulk modulus

G: Shear modulus

Kf: Bulk modulus of pore fluid

Ks: Bulk modulus of solid grain

Kfr: Bulk modulus of drained rock

R: Sphere radius

$\delta$: Delta (Displacement)

$\lambda$: Lambda (wavelength)

$\varepsilon$: Strain

$\eta$: Eta (Energy coefficient)

$\phi$: Porosity

$\pi$: Pi (Mas density)

$\sigma$: Stress

$\rho$: Density

$\alpha$: Relative displacement

$\sigma_p$: External hydrostatic sphere

# Table of Contents

# List of Figures

# List of tables

# Chapter 1: Introduction

## 1.1. General Introduction:

Most of the energy we used today is fossil based which are oil, gas and coal. However it can be defined more broadly such as Nuclear (Uranium) and hydroelectric power can also be the source of energy. Since the oil was first discovered in 1860's it becomes very attractive to the world and today's 85% of the world's energy we are using is based on hydrocarbon fossil fuels. With time things are changing as the consumption of oil and gas increasing continuously. For those new techniques of exploration, production improvement, recovery of hydrocarbons and safe drilling demands more enlightened and advance technology for better understandings of subsurface structures. New technical advancements in laboratory experimental research on reservoir characteristics behavior in subsurface has been done which contributes for better understandings.

This thesis work is the continuation or extension of the project carried out by the writer in the previous semester project. So some of the theoretical research data and experimental procedures were rewritten in the present research work as it has a link with the present thesis report. However none of the experimental data has used in the present studies.

The main motivation of the research was the literature and experimental study of the compressional and shear wave velocity (P-and S-wave velocity) ratio, behavior with different fluids and with different grainsized sand samples by using Biot-Gassmann equation which is widely accepted in oil industry for sand and sandstones. The task was to find how we can use the rock physics to build a relationship between both geology and geophysics. As the seismic properties changes as a function of geological texture and fluids and for that it is very essential to know the compressibility and stiffness of the rock and pore space. Present studies have been made on the unconsolidated reservoir to see the possible effect on velocities because of the different grain sizes, sorting and fluids.

Parsad (2002); Domenico (1977); and Zimmer (2003) have investigated the velocities behavior with respect to the stress in unconsolidated sand. The present study is aiming to contribute to the basic understandings of velocities as a function of external stress in various sand samples with different grainsizes and different percentage of brine. All the data presented graphically in Chapter 4, illustrates the effect of brine, grainsize and stress on velocity. In addition, an attempt is taken to explore the Strain and porosity behavior with stress. Finally, some seismic attributes like Vp/Vs are shown to demonstrate the characteristics of different lithology in laboratory measurements.

## 1.2.  Motivation and research objectives:

The main motivation of the present research was to find the seismic velocities behavior with respect to different grain sizes, pore pressure and different percentage of fluids (brine), by using the knowledge of seismic, reservoir geology and most importantly rock physics. For the basic understanding of the velocities as a function of external stress and pore pressure in various sands samples with different grain sizes have been investigated in the lab in an Oedometric setup to measure:

- Effects of external vertical stress on velocities.
- Effects of fluids on velocities.
- Mineralogical effects on velocities.
- Effects of vertical stress on strain.
- Effects of vertical stress on porosity.

## 1.3.  Chapter Description:

**Chapter 1** contains the general introduction and a short description of the motivation and research objectives.

**Chapter 2** includes the theoretical background, poroelastic theory, fluid substitution, grain contact theories, stress sensitivity, change in porosity, effective stress for velocity and geological aspects of sand. This chapter also reviews the previous experimental work on inconsolidated sand with special emphasis on velocity, strain, porosity and Vp/Vs with their relation with stress.

**Chapter 3** explains the experimental setup, sample preparation and test procedure.

**Chapter 4** demonstrate the experimental results and analysis of the data with the focus on change in vertical P-and S-wave velocities with stress with change in grain size, sorting and fluid substitution.

**Chapter 5** gives the conclusion of the important findings of the present work and recommendation of the future work.

# Chapter 2: Theoretical and experimental background:

Rock composition is determined by the percentage of the elements and constituent minerals and elements contained within it. So a rock body consists of a solid frame with a pore spaces within it. Elastic/acoustic behavior is affected by the change in rock structure. Acoustic properties of the rocks are depends on the porosity, mineralogy, pore fluid, pore geometry, pore pressure, overburden (Stress), change in cementation etc. In an oil industry it is widely accepted to use Biot-Gassmann equation for fluid substitution in sand and sandstone. The present chapter will reviews the theoretical and experimental behavior of the parameters which are discussed above and also the velocity affects in unconsolidated sands (weathered layers). Moreover, some geological aspects of sand and previous experimental results are also included at the end of this chapter. To understand this fluid substitution concept Biot-Gassmann poroelastic theory is also discussed below as for understanding of the writer.

## 2.1. Biot's Poroelastic theory:

Poroelasticity is a continuum theory for the analysis of porous media composed of an elastic matrix containing interconnected fluid saturated pores. Physically terms, the theory process that when a porous media subjected to stress, the resulting matrix deformation leads to the deformation leads to volumetric changes in the pores. As the pores are filled with fluids so the presence of the fluid not only behaves as a stiffener of the material, but also counts in the flow of the pore fluid between high and low pressure belt.

Mechanical behavior of the rock mass is influenced by the composition of the rock body. So when the sediments deposited e.g. sand and clay they show very high porosities. With the time when these sediments subjected under compression (stress) their porosities get lower. Naturally these sediments filled with cracks and pores that are saturated with one or more fluids. With depth due to increase in overburden stress fluid in the pores starts to escape and creates the pore fluid pressure. These pore fluids results the elastic deformation of the rock [1]. This movement of the pore fluid in the rocks is not only because of the response to the gradient in pore pressure, but can also escape due to the tectonic forces. Thus, the mechanical behavior of the rock is fully coupled, even though some analysis of the mechanics problems, and subsurface flow problems, disregard this coupling [2].

Coupling between changes in stress and change in fluid pressure forms the subject of poroelasticity. Two basic phenomena describe the poroelastic behavior.

- Fluid to solid coupling occurs when a change in fluid pressure or fluid mass produces a change in volume of porous material.
- Solid to fluid coupling occurs when a change in applies stress produces a change in fluid pressure or fluid mass. [3].

Theory of the poroelasticity accounts for this coupled hydro mechanical behavior. Theory was chiefly put forth by Biot [4], and developed further by, among others Detournay and Cheng [5].

For the present study Biot's Gassmann theory will be summarized for the better understanding of the velocities behavior within rocks with fluids.

## 2.1.1. Fluid Substitution:

Gassmann, 1951 predicts that how the rock modulus changes with the variation of the pore fluid. In fluid substitution estimation two fluid effects are considered which are the change in rock bulk density and rock compressibility.

The compressibility of the dry rock can be defined as the sum of the mineral compressibility and an extra compressibility due to pore space as follows:

$$\frac{1}{K_{dry}} = \frac{1}{K_{mineral}} + \frac{\phi}{K_{\phi}} \quad\text{................................................2.1}$$

Where, $\phi$ is the porosity, $K_{dry}$ is the dry bulk modulus, $K_{mineral}$ is the mineral bulk modulus and $K_{\phi}$ is the pore space stiffness. In a same way compressibility of a rock saturated with a fluid is define as:

$$\frac{1}{K_{sat}} = \frac{1}{K_{mineral}} + \frac{\phi}{K_{\phi}+K_{fluid}.K_{mineral}/(K_{mineral}-K_{fluid})} \quad\text{........2.2}$$

Where, $K_{fluid}$ is the pore fluid bulk modulus. Gassmann equation by further solving Eqs, 1.1 and 1.2, can also be written as:

$$\frac{K_{sat}}{K_{mineral}-K_{sat}} = \frac{K_{dry}}{K_{mineral}-K_{dry}} + \frac{K_{fluid}}{\phi(K_{mineral}-K_{fluid})} \quad\text{..........2.3}$$

and,
$$\mu_{sat} = \mu_{dry} \text{.....2.4}$$

Therefore Eqs, 2.3 and 2.4 predicts the modulus for an isotropic rock where the rock bulk modulus will change if the fluid changes, but the shear modulus will not change. The dry and saturated moduli are related to P-wave velocities as:

$$V_p = \sqrt{\frac{K+\frac{4}{3}G}{\rho}} \quad\text{..................................................2.5}$$

For the S-wave. Equation we have is:

$$V_S = \sqrt{\frac{G}{\rho}}$$.................................................................2.6

$$G = G_{fr}$$.................................................................................2.7

Where, G is the shear modulus, Gfr is the shear modulus of the rock frame and $\rho$ is the density. Here in this case velocity will have the inverse relation with the density and density will be denominator will have a dominant effect on the above expression. So the S-wave velocity in the fluid saturated rock will be lower because there will be no fluid effect on the shear modulus.

## 2.1.2.   Assumptions:

- Isotropic material behavior.
- Porous and permeable.
- Homogeneous.
- Linear elasticity.
- Complete saturation with brine.

# 2.2. Stress Sensitivity:

Materials properties like velocity and strain are sensitive to stress because of the possible sources which are:

- Change in porosity
- Presence or generation of cracks/fractures
- Existence of sharp grain contacts

## 2.2.1.   Change in Porosity:

Porosity is normally reported as the percentage of the total volume of the rock or porosity is the measure of the void space in the reservoir rock. Based on these void spaces porosity can be between the grains (interparticle) or within the grains (intraparticle). Porosity can be primary (sedimentary) or secondary (diagenetic). [6]

Sands and shales both show very high porosity at the time of deposition. At the time of deposition porosity gain by the sediments is primary porosity. Due to the further depositional processes of the sediments, porosity starts to reduce because of the overlying sediments which results cementation of the sediments called secondary porosity. Factors involves in the decrease in porosity are increase in grain size, increase in grain packing and shape, decrease in sorting etc. These factors are dependent on the composition of the rocks from which the sediments are derived (source rock), transport mechanism, transport length and chemical and physical processes acting on the sediments during burial (digenesis).

The Stress in the rock material increases as the increase in weight of the overburden with depth. This results the compaction and fluid in the pores starts to escape because the sediment is subjected to subsidence and consequently reducing its pore space to accommodate with the new stress condition. It is very necessary to relate the change of porosity with stress (depth), in order to understand the stress sensitivity of rock material properties.

According to the Biot poro-elastic theory the following relation can be used to explain the change of porosity with applied stress by using the effective stress law,

$$\frac{\Delta\emptyset}{\emptyset} = \left(\frac{\alpha}{\emptyset} - 1\right)\Delta\vec{\sigma}/Kfr \dots\dots\dots\dots\dots\dots\dots\dots\dots\dots\dots\dots\dots\dots\dots\dots2.8$$

Where $\phi$ and $\Delta\phi$ is the absolute and the corresponding change of porosity, $K_{fr}$ is the frame modulus of the sample, $\Delta\vec{\sigma} = \frac{\sigma_1+\sigma_2+\sigma_3}{3} - P_f$ mean effective stress and

$$\alpha = 1 - \frac{K_{fr}}{K_S} \text{ Biot Coefficient } \dots\dots\dots\dots\dots\dots\dots\dots\dots\dots\dots\dots\dots\dots\dots2.9$$

This relation validity is only in linear pore-elastic condition where $K_{fr}$ is constant. The effective stress law is valid only when the velocity is sensitive to applies stress. These parameters can be found by using the hydrostatic stress setup in the laboratory. However, except for small

changes in porosity , stress dependence of the wave velocity requires a non-linear stress-strain relation.

To see this possible effect on porosity due to overburden stress (primary porosity) and this effect on Vp/Vs ratio will be further evaluated graphically in report.

## 2.2.2.    Grain contact theories:

Acoustic wave's propagation in earth material controlled by the properties like solid frame of the material.  Grain contact provides the better understandings of the frame properties [7]. Hertz solved the linear elasticity equations for elastic bodies in contact. (Hertz 1881; Timoshenko and Goodier, 1970; Johnson, 1985). The resulting static force displacement relation for displacement along the line of centers between two contacting, identical spheres is given by [8]

$$F = \frac{1}{3}\frac{E}{1-v^2}\sqrt{2R\alpha^{\frac{3}{2}}} \dots\dots\dots\dots\dots\dots\dots\dots\dots\dots\dots\dots\dots\dots\dots2.10$$

Where, E is the Young's modulus, $v$ is the Poisson's ratio, R is the spheres radius, and α is the relative displacement after initial contact.

## Hertz & Mindlin theory

Hertz introduced the grain pack model presuming linear elastic grain material where contact radius is much lower than the grain radius. Theory provided the shear and bulk modulus assuming no slip between the spheres. Hertz theory is restricted to frictionless surfaces and perfectly elastic solids. But later in the century progress in the contact mechanics has been associated with the removal of these restrictions [9]. Later, Mindlin (1949) established the theory based on Hertz (1882) which explains the longitudinal and shear force constant acting on the contact.

## Walton Theory

Walton and Hagen (1984) calculated the response of an elastic spheres impacting a rigid wall using finite element code (Halquist, 1978) [10]. Lter Walton (1987), considering the possible slip (smooth spheres) and no slip (rough spheres) conditions at the contact surface has derived two sets of equations. Walton (1987) has derived the effective bulk and shear modulus for the random packing of same size spheres (φ≈0.36) under pre-strain, where wave induced stresses are small (Hertz-Mindlin contact low applied to all constants). The derived equations for both non slip and perfect slip (rough) conditions are:

$$K = \left[ \frac{n^2(1-\phi)^2 G_s^2}{18\pi^4(1-V_s)^2} \sigma_p \right]^{1/3} \quad \text{................................................................2.11}$$

$$G_{smooth} = \frac{1}{10}\left[ \frac{12n^2(1-\phi)^2 G_s^2}{\pi^2(1-V_s)^2} \sigma_p \right]^{1/3} = \frac{3}{5}K \text{..........................................2.12}$$

For a rough Sphere,

$$G_{rough} = \frac{5-4V_s}{5(2-V_s)}\left[ \frac{3n^2(1-\phi)^2 G_s^2}{2\pi^2(1-V_s)^2} \sigma \right]^{1/3} \text{.................................................2.13}$$

Where, K and G are the effective Bulk and Shear Modulus, $V_s$ is a Poison ratio of solid grains and $\sigma_p$ is the external hydrostatic stress for a dry rock. [11].

## Assumptions:
- Contact porosity
- No new contacts are assumed to be generated, so coordination number is constant.

# 2.2.3. Effective Stress for Velocity:

Compressional and shear wave velocities are related to the effective stress that subjected onto the material of interest and can be expressed as $V_{p,s=(\sigma_p)}$, where $\sigma_p$ is the effective applied stress. This effective stress is related to the applied external stress and pore pressure in the material. So the above mentioned relation can be written as $V_{p,s=f(\sigma,P_p)}$, [12], which can be used to predict the distribution of pore pressure in the subsurface [13]. So for the relation of both external stress and pore pressure to

calculate the effective influence of stress on a material we need a combine equation. Terzaghi was the first who introduce the effective stress concept in 1923 based on the empirical studies. In that he assumed that by increasing the external hydrostatic pressure produce the same volume change of material as reducing the pore pressure with the same amount and shear strength depends only on difference between normal stress and pore pressure. This concept leads to the formulation of Biot coefficient, which describes the stress coefficient for strain.

$$\sigma_p = \sigma - \alpha p_f \dots\dots\dots\dots\dots\dots\dots\dots\dots\dots\dots\dots\dots\dots\dots\dots\dots\dots\dots 2.14$$

Where, $\sigma_p$ is the effective stress acting on the material under external hydrostatic stress $(\sigma_p)$ at certain pore pressure $(p_f)$. $\alpha$ is the effective stress cofficent which can be determined by using the formula,

$$\alpha = 1 - \frac{K_{fr}}{K_s} \dots\dots\dots\dots\dots\dots\dots\dots\dots\dots\dots\dots\dots\dots\dots\dots\dots\dots\dots\dots\dots 2.15$$

This $\alpha$ is commonly used to calculate the effective stress coefficient for strain.

## 2.2.4. Geological Aspects of Sand:

Sediments have accumulated during a particular time period at a significantly greater rate (Ulmishek & Klemme, 1990). The history of the deposition of these sediments is very long. Mostly the deposited sediments in the basin are Sand and Clay. Main process involves in deposition of these sediments are weathering, Erosion, transportation and finally the deposition. Each of the sediments has their own source rock from which they weathered and eroded. These source rocks can be igneous, metamorphic or sedimentary.
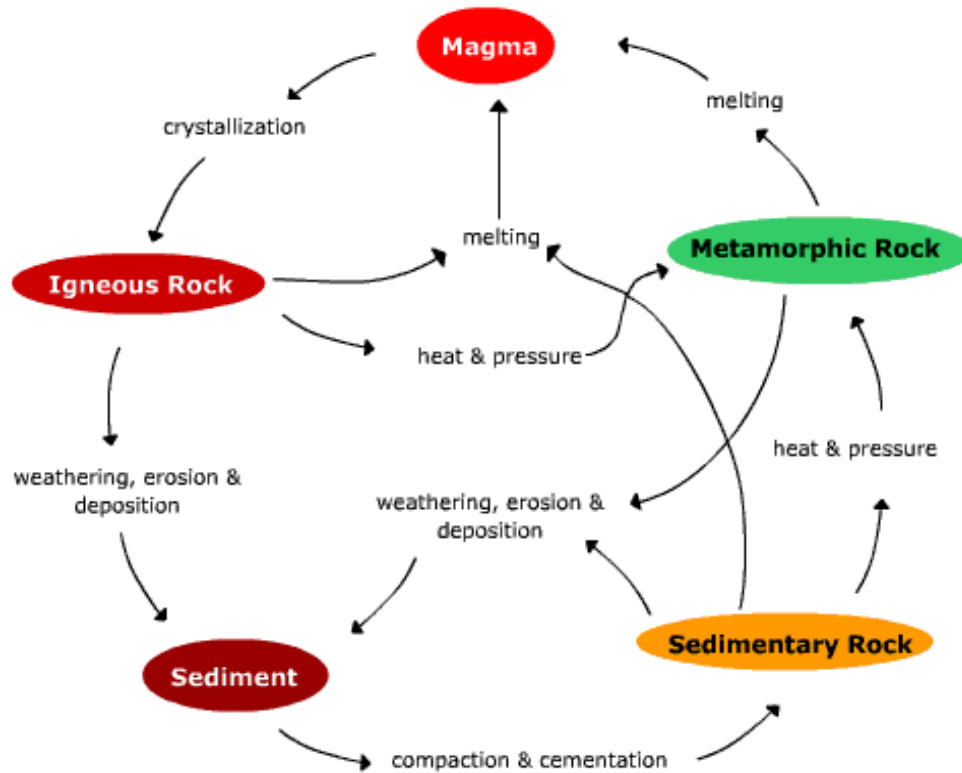


**Figure 2. 1 Rock cycle model [14]**

To understand the depositional processes and geological aspect of sand which are involves in changing of an earth's crust we have to understand the processes that involves in these changes. The main processes involves are weathering and erosion. In weathering rocks decomposes into small pieces which can be chemical or biological. After weathering of the rocks with the action of water (rain, river, and ocean), wind or gravity these decomposed material transported and deposited in a different environments which are called depositional environments. These environments could be fluvial, alluvial, marine, deltaic, lake deposition etc. These depositional environments are very important for the recognition of the mineral originality.

Sandstone mostly consists of sand grains. Sand itself used to describe the grain size which depends on the composition, source rock and the agents which involves in the transportation. Sandstone is characterized by texture and composition which involves sorting and rounding.  Sorting refers to the size

distribution of grains and rounding of the grains from abrasion reflects the energy during transport and depositional environment. Sand can be distinguished from other sediments depending on their grain size. Normally sand grains are 0.063-2mm in size. Texturally sand grains are stable that's why sandstone reservoirs hold good potential for hydrocarbon accumulation because of good porosity and permeability.

The main purpose to discuss sand depositional history and effect on sand composition due to different depositional environments was, as most of the potential reservoirs are sandstone. To understand the reservoir characteristics behavior in subsurface, laboratory experiments were done on different grain sizes and sorting of sand samples to see the possible changes in seismic velocities (Vp/Vs). Also to see the possible effects on Vp/Vs with interaction of different sand samples with different fluids were measured and will be discussed further in the report both graphically and theoretically.

## 2.3.  Experimental Background:

Domenico (1997) perform an experimental study on unconsolidated brine and gas saturated sand (Ottawa sand) and glass beads which shows nearly identical porosities to calculate the effect of the compressive stress and pore fluid properties on elastic properties of unconsolidated sand. He observed that the S-wave velocity for both brine and gas saturated specimen and P-wave velocity for gas saturated specimen were increased $\frac{1}{4^{th}}$ power of differential pressure. He also found that the replacement of the gas with brine show as increase in P-wave velocity and reduces with the rate of increase in pressure.

Parsad (2002) investigated that the Vp/Vs and Qp/Qs (ratio of the attenuation of P-and S- waves ) ratios can be helpful in the investigation of lower differential pressure and can be used as indicators of zones with overpressure. She observed that the ratio of the Vp/Vs at low effective pressure decreases rapidly with pressure. She also observed that the ratio of the Vp/Vs show very high in at low differential pressure for unconsolidated sands, which decreases with increase in differential pressure.

An empirical relation has been derived for the change in Vp/Vs with pressure which is:

$$\frac{Vp}{Vs} = 5.6014 P_{d}{}^{-0.2742} \dots\dots\dots\dots\dots\dots\dots\dots\dots\dots\dots\dots\dots\dots\dots\dots\dots\dots\dots\dots\dots 2.16$$

Where, Vp and Vs are the P and S wave velocity and $P_d$ id the differential pressure.

Huffman and Castagna (2001) and Parsad (2002) have demonstrated the Vp/Vs ratio as the indicator of pressure. They calculated the P- and S-wave velocities through sands and glass bead at a range of porosities and by using Vp/Vs in unconsolidated sand they evaluate the pore pressures. They also calculated the porosity from the grain density, dry sample and sample volume. They measured the changes in volume of the sample and porosity with pressure by measuring the changings in length and circumference of the sample. Porosity error was estimated about 0.02%.

# Chapter 3: Experimental Methods

The experimental study carried out for this master project consists of small scale laboratory tests on oedometer setup by using Biot-Gassmann equation for fluid substitution in sand and sandstone. As this project is a further continuation of the previous project done by the writer as discussed above in chapter 1. For this purpose in first case (01) all the samples were saturated with 3.5 wt% sodium chloride to imitate the subsurface conditions. While in second case (02) different tests were performed on pure sand with different grain sizes to see the possible effect of grain size and fluid effect on velocity at different stress levels. To understand that variation four different grain sized samples were used. Ottawa GS# 30-70, Ottawa GS# +450, Colombia GS# 30 and Columbia GS#550-450. The sample description is given in Table 3.1.

In addition three different tests were performed on a same sized, Ottawa GS#30 with different percentage of brine to see the possible effect on velocities. Sample description and brine percentage is given in table 3.2.

This chapter reviews the oedometer setup and its components (LVDT's) and Quisix pump (pore pump) that were used during experiments were described. Moreover sample preparation method is also explained. Further acoustic system and procedure of the data processing are explained. Later measurement of stress, strain, porosity and density are also discussed. Finally there is a section to describe the uncertainties of parameters measurements.

## 3.1. Oedometer Setup:

The Oedometer shown in Figure 3.1 was designed by Morten Ivar Kolsto (Phd student). Later it was further modified by another Phd Student Muhammad Hossain Bhuiyan. It was used for testing the elastic and acoustic properties of the sand or clay mixtures under uniaxial strain conditions. The thing which makes this oedometer setup prominent then the popular used oedometer cell is the possibility to measure both vertical and horizontal P-wave in combination with a vertical S-wave.

We can divide the complete test apparatus into two setups: An internal and external setup. The internal setup consists of: a) A main chamber, b) A piston, c) A load frame. Main chamber and piston are made of stainless steel material. The most prominent part of the main chamber is the sample holder which has a diameter of 69.90mm, a height of 40mm and is located in the middle of the main chamber. The thickness measured from the wall of the sample holder to the outskirt of the main chamber of the outer ring is 50.00mm to make sure negligible lateral strain during tests. Sample is loaded from top to bottom. There are two fluid flow channels connected to the base of the sample holder. And two additional connected to the piston part of the internal setup. One of these two channels is an injection channel connected to the Quisix pump. A 3.00mm thick filter made of stainless steel and with a specific filtering capacity is 0.5μm is placed below the upper drainage and above the lower drainage channels. A second paper filter with identical properties is placed beneath the steel filter for complete sealing at the base.

Silica gel is filled in the areas outside of the steel filter. It must be emphasized that the contact area for this particular sealing is small making it possible to apply desired stress ≈10.0 MPa during tests.

Beside this there are some acoustic devices mounted at the center of the sample holder base used to control different measurements. This device consists of the piezoelectric P-and S-wave transducers with a center frequency of 500 kHz in associated with a peek from piece with a diameter of 35.00 mm. To reduce the acoustic impedance between the unconsolidated samples specifically the material for the front piece is chosen and the front piece down to minimum. This generates signals that are easy to detect even for low stress level, which is important for velocity estimation. P-wave velocity of the peak is 2563 m/sec.

To exert load from the load frame onto the sample, piston is used to decorated with both the same type of filter and drainage at the base of the sample holder with the identical acoustic device in the center (Figure 3.1).
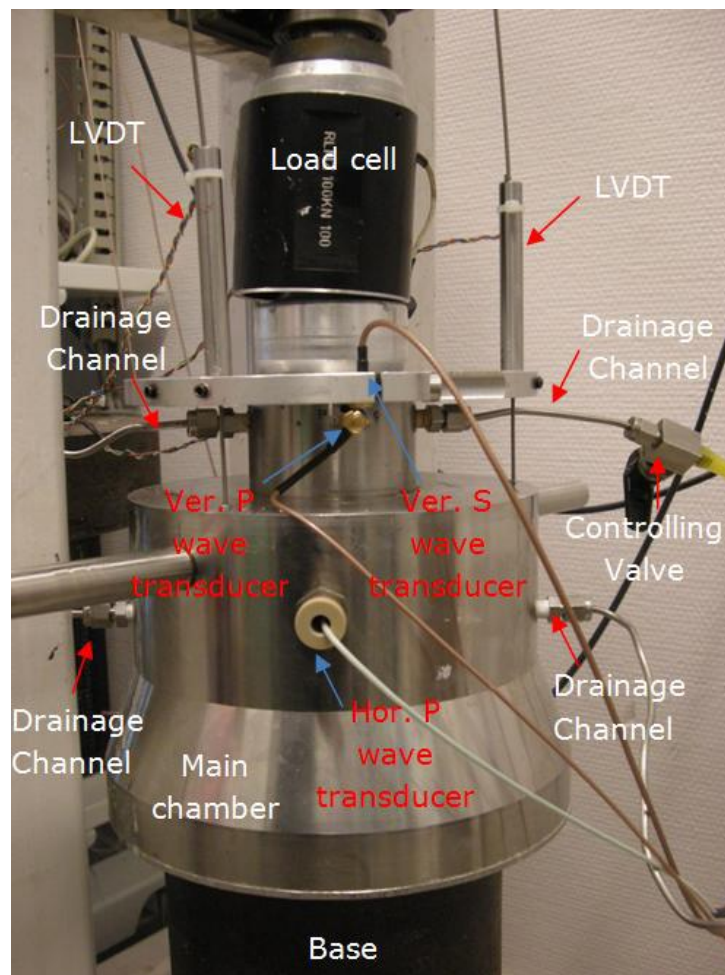


**Figure 3. 1 Basic setup for oedometer cell [15]**

For the sealing two O-rings are used. The first O-ring is mounted around the piston to prevent the slurry to penetrate under the filter accessing the drainage channels. Between the first O-ring and the sample

holder wall down to minimum, the O-ring is gently lubricated with a thin oil film in order to reduce the friction.

To create the external stress on the sample the load frame is used. For exerting stresses through a thick steel rod a set of about 25kg dead weight are used in one end of the lever and a load cell mounted on the top of the piston Figure (3.2) and (3.3). As a lever is used, the stress level will vary during a loading due to the compaction of the sample. Thus, to be able to control the stress change the system need to be calibrated with the lever piston for the particular dead weight. Prior to the tests and estimates this calibration was conducted and estimates the conversation factor from Volt to kN.
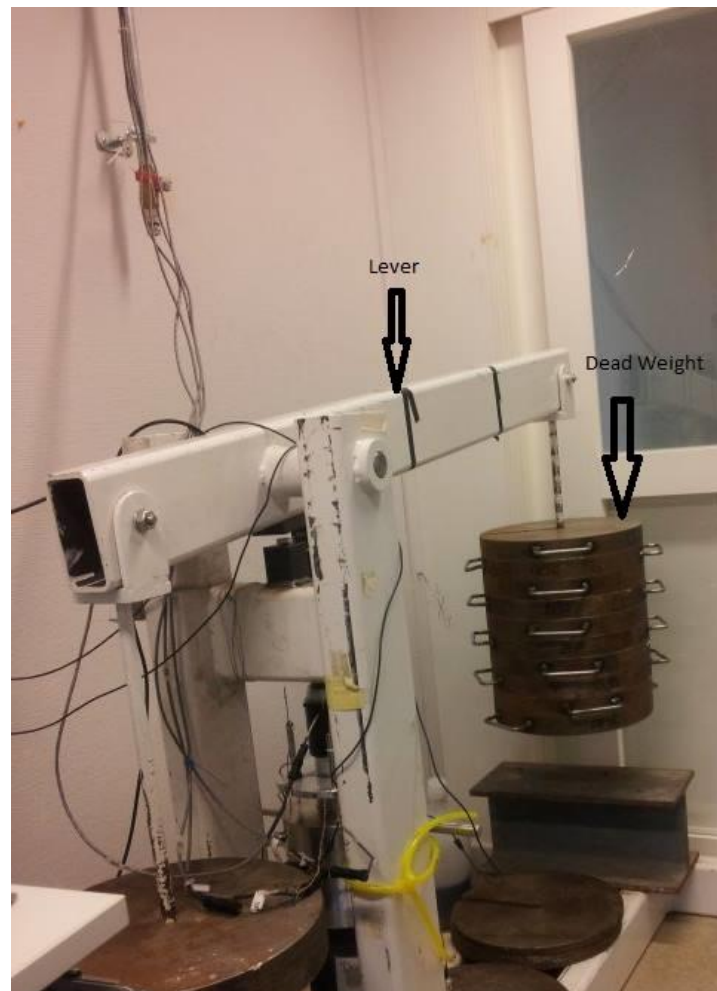


**Figure 3. 2Load frame of the oedometer setup [16]**

In the oedometer cell the external setup consists of: a) Device measuring the compaction of the sample during the test with a software and acquisition setup; b) acoustic acquisition setup and c) pore pump which is used to obtain the desired water pressure applied on the sample (Figure 3.2). It contains two pumps that keep the desired programmed pore pressure adjusting alternatively by receiving or delivering the pore fluid.

## 3.2. Linear variable Differential transformers (LVDT's):

A device called Linear Variable Differential Transformers (LVDT) measures the change in length of the sample very accurately and precisely. To measure the compaction on different part of the sample surface three LVDT's were used. To find out the range of the measurable length change is estimated about 10-12 mm. An acquisition station monitors and acquires the uniaxial compaction and applied stress data. The length change estimated by the amplifier and stress according to the calibration data provided to the software Figure (3.3).



**Figure 3. 3 Acoustic compaction and stress data acquisition setup in an oedometer [17]**

## 3.3. Sample preparation:

In order to perform experiment different samples of dry and saturated pure sand with different grain sizes were collected for the first case. For second case sample with same grain size but with different percentage of brine were prepared in order to measure the expected results. Before the experiment samples were prepared very carefully in order to achieve the best possible results by performing the possible steps:

- All the samples were put in the oven for the whole night at 110˚C before using for the test in order to keep the sample completely dry.
- Before using the samples were put in a room conditions for about 20 minutes to keep it cool.
- All the samples were weighted before using for the test to make sure how much exactly will be used of test.
- To get the weight of the samples each of the samples was weighted on a weighing scale within a plastic jar. Weight of the empty jar was taken before by following the same procedure on scale.
- Volume of the each sample was calculated by calculating the radius of the sample holder and with density in cm3.
- In order to get the exact amount of sample, the sample was poured very carefully into the sample holder without any loss of the sand.
- After putting the sample in sample holder, it was made sure that the sample has a contact with piston.
- For making the brine for each case few grams of sodium chloride with water were mixed with in beaker. For 3.5wt% of brine case, 10.88gm of sodium chloride were mixed with a 300gm of water by using the following formula:

$$Wt\% \ NaCl = mass \ of \ NaCl/mass \ of \ NaCl + water$$

- Same procedure for making different percentage of brine was used for keeping the percentage of the brine high for different cases.
- Sample description and brine percentage is given in table 3.1 & 3.2 respectively.

**Table 3. 1 Showing the sample composition used in the test in oedometer setup for case#01**

| Case#1 | Sand Sample | Sand (Vol %) | Brine Saturation | Grain sizes (mesh size US) |
|---|---|---|---|---|
|  | Ottawa Dry + Saturated | 100 | 0 | 30-70 |
|  | Ottawa Dry + Saturated | 100 | 3.5 | 30-70 |
|  | Ottawa Dry + Saturated | 100 | 7 | 30-70 |

**Table 3. 2 Showing the sample composition used in the test in oedometer setup for case#02**

| Case#2 | Sand Sample | Sand (Vol %) | Brine saturation | Grain sizes (mesh size US) |
|--------|-------------|--------------|------------------|----------------------------|
| | Columbia Dry + Saturated | 100 | 3.5 | 30 |
| | Columbia Dry + Saturated | 100 | 3.5 | 550-450 |
| | Ottawa Dry + Saturated | 100 | 3.5 | 30-70 |
| | Ottawa Dry + Saturated | 100 | 3.5 | +450 |

## 3.2.1.   Precautions:

- All the samples were carefully weighted before using for the test in order to avoid any loss of the material and to make the measurements more precise.
- Before starting an experiment every single parameter were checked to get the best possible results.
- For the saturation brine was carefully weighted and mixed in a weighted percentage of water in order to get the accurate mixture of brine.
- It was difficult to get the constant stress interval due to the movement of the lever arm, but still the loading and unloading was done very carefully in order to avoid the technical problems.
- Before putting the load contact between the sample and piston was carefully observed.
- By using Vernier caliper piston height was carefully measured by using the inside jaws to get the exact diameter of the piston height from different positions.
- Putting the dead weight of 25 kg was the huge safety issue. So during both loading and unloading it was done very carefully to avoid any of the laboratory damage.

# 3.3. Test Description:

Al the tests were performed in an oedometer setup is typically in uniaxial compaction test. The test plan had two main sequences. In the first main sequence the pore pressure was kept constant at the 1.0 MPa while the external stress was increased step by step from ≈ 25.0 kg, is equivalent to ≈0.7 MPa. In reducing the external stress, to end the first main sequence an equivalent unloading cycle were performed as shown in Figure 3.4. These sequences were used to simulate a compaction and decompression event within and around a shallow reservoir. This loading and unloading cycle resembles the sediments compaction and with burial depth and reduction of overburden stresses can be due to the erosion uplift which could be because of any tectonic activity. The Loading and unloading cycle shown here in Figure 3.4 is just for the first case with 3.5 wt % salanity. For rest of the samples test plans are presented in the Appendix A.
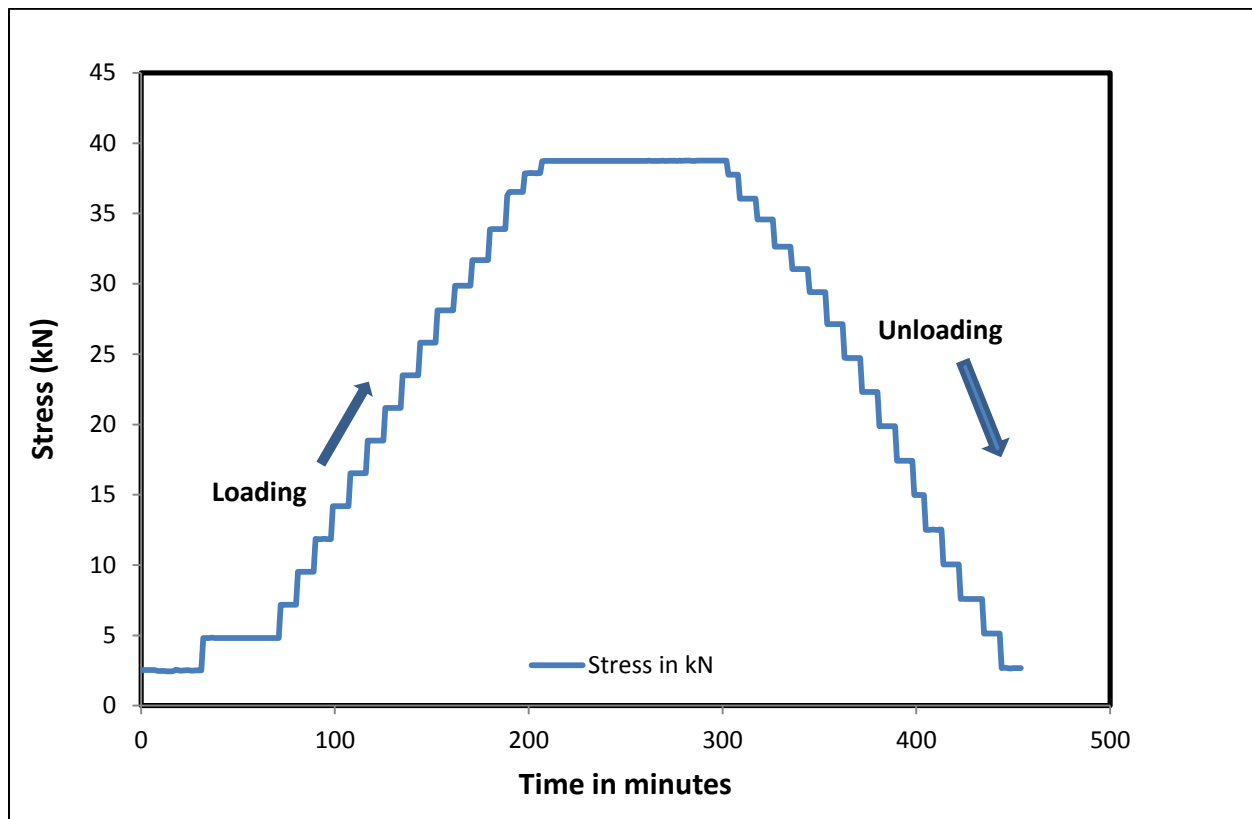


**Figure 3. 4 Showing the loading and unloading cycles for OT (3.5 wt %)**

# 3.5. Acoustic configuration and data processing:

Acoustic devices attached to the center of the sample holder base in order to control the different measurements. To find the best frequency that shows the high amplitude signal with low attenuation, several frequencies were used. For the vertical P-wave, 500 and 400 kHz were chosen and for the S-wave 130 and 110 were used. Vertical P-wave signals at 400 kHz were observed best while the S-wave signals at 150 kHz were seems to be good. Figure 3.5 shows the position of velocity picking for both P- and S- wave respectively. For P-wave first zero crossing was used to pick velocities while for the S-wave second zero crossing was used. Horizontal P-wave was not showing some time because of some technical issues. The signal gathered during the experiments for each of the test and frequency difference between the calibrations was corrected for the sample travel time. Measurement of the travel time through the transducers and peek front was measured by peek sample which has the acoustic properties already well measured.
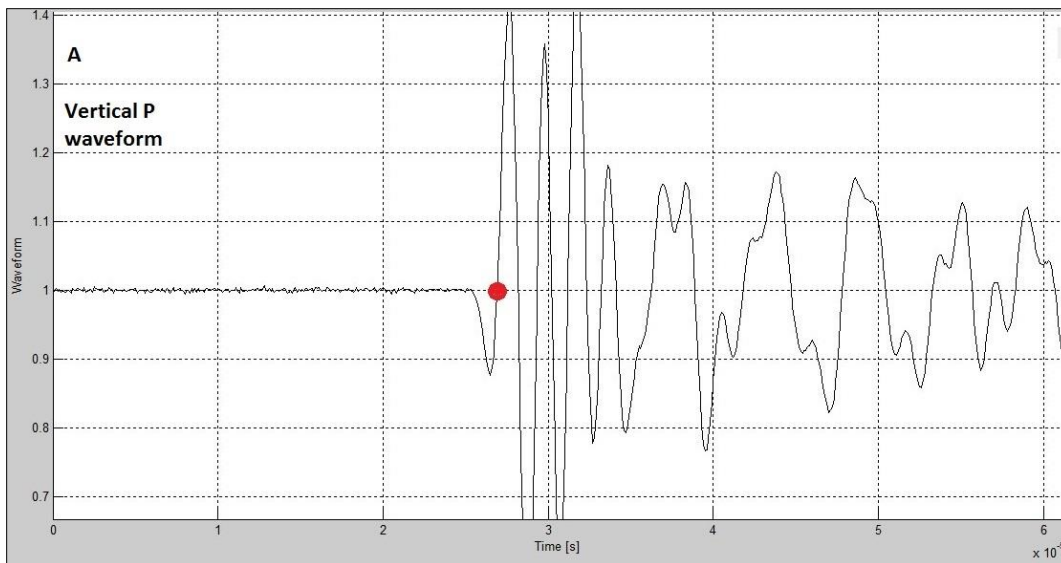


**Figure 3. 5 Showing waveform for vertical P-wave. Red circle showing the picking of the position of the travel time [18]**
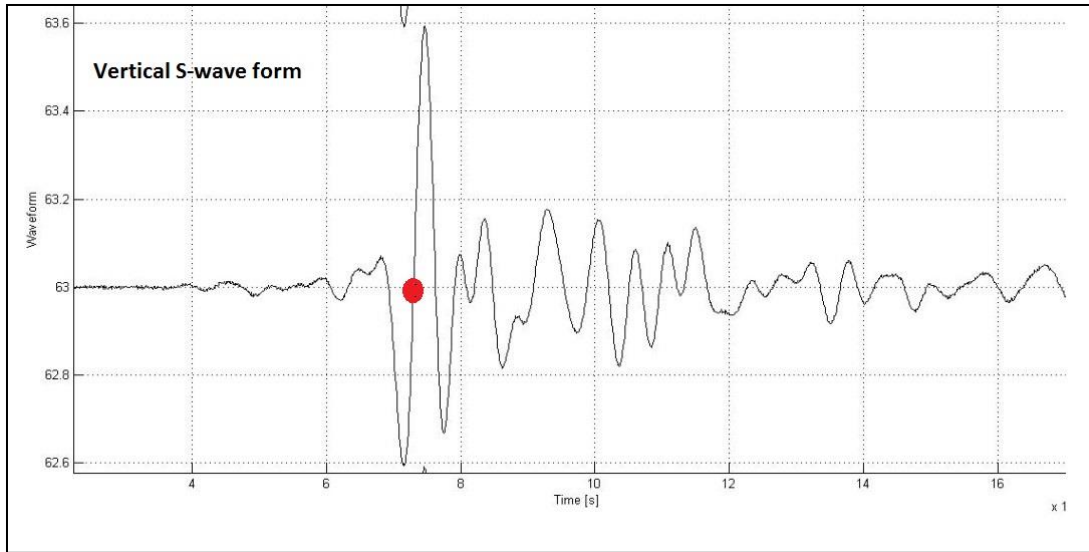
**Figure 3. 6 Showing waveform for vertical P-wave. Red circle showing the picking of the position of the travel time [19]**

## 3.4. Stress and Strain Measurements:

All the tests were performed in an oedometer setup in a uniaxial compaction test. For the measurement of the stress during tests, dead weight of ≈ 25.0 kg, which is equivalent to ≈0.7 MPa, were applied for each step until the stress increases reached up to ≈10.0 MPa. The idea was to calculate the compaction and decompression within a shallow reservoir by loading and unloading cycle by applying the stress in a sequence. The first loading cycle was achieved by exerting the stress in a sequence until the external stress reached 10.0 MPa and with the same procedure unloading was done.

For measurements of strain initial sample length was measured. LVDT's and load cell was switched on in order to know how much sample length change in correspondence with the stress increment. This change in length at every stress level was automatically recorded on the LVDT's data setup for each incrimination. This process was monitored for each of the test. To make the measurements more précised initial length was measured very carefully at different points in order to avoid error estimation.

## 3.5. Porosity Measurement:

For the porosity measurement, initial porosity $\emptyset_i$ was calculated by using the following formula.

$$\emptyset_{i=\frac{V-Vs}{V}}\dots\dots\dots\dots\dots\dots\dots\dots\dots\dots\dots\dots\dots\dots\dots\dots\dots\dots\dots\dots\dots\dots\dots\dots\dots\dots\dots\dots\dots\dots\dots\dots.3.1$$

$$Vs = \frac{m}{\rho}$$

Where, V is the total volume of the sample, Vs Is the solid volume; m is the mass of dry sand grain and $\rho$ is the density of the sand.

For the calculation of the total volume, total piston height was measured before, radius of the oedometer sample holder was known and the height of the chamber was measured by using a slide caliper. For the initial porosity measurement, individual mass of the dry sample was measured very precisely.

To find the changes in porosity due to compaction of the sample during test were estimated by comparing this change in volume of the test sample by using LVDT's which is dependent on the stress.

## 3.5.1.    Error estimation:

Although the measurements were taken very carefully but still experiments contain errors. To minimize these errors by taking extra attention to choose the correct instrumentation and measure the data very precisely.

The error estimation was done both manually and mathematically.

## 3.5.2.    Manual:

- Theses error measurements were done to estimate the error for the external stress on the sample.
- For the compaction measurements LVDT's data used.
- Sample volume due to uncertainties of the measured lengths and radius of the sample.
- Travel time picking through the sample depends on the change in frequency between received calibrated signal and the signal received during test.

The calculated uncertainty in the relative compaction of the sample is ±0.03 mm. the measurement uncertainty because of the possible friction occurring between the piston and sample holder in the applied load is of ±0.01 kN. Radius and initial sample length were measured within ± 1.0 gm. The uncertainty in the density is estimated to be ±0.054 gm/cc. For the travel time error estimation due to the change in frequency in the test and calibrated signal are calculated to be for vertical P- and S- wave, 0.33 $\mu_s$ and 2.14 $\mu_s$ respectively.

## 3.5.3.    Mathematical:

### Porosity Uncertainty Calculation:

Error estimation for both porosity and velocities were estimated by using the same formula as used by the Hornby (1998).

Porosity of the sample for different samples was calculated by using expression:

$$\emptyset = \frac{V - Vs}{V}$$ ...............................................................................3.2

Where, Ø is the calculated porosity, V is the total volume and Vs is the solid volume. Total volume is given as:

$$V = A.L \text{..................................................................................} 3.3$$

$$A = \pi r^2 \text{..............................................................} 3.4$$

Where, A is the area, r is the radius of the sample holder and L is the length of the sample.

By considering the length, density and mass measurements, error estimation was done by the expression below is evaluated by considering the parameters mentioned above as:

$$\Delta\phi = \frac{\delta\phi}{\delta m}\Delta m + \frac{\delta\phi}{\delta\rho}\Delta\rho + \frac{\delta\phi}{\delta A}\Delta A + \frac{\delta\phi}{\delta L}\Delta L \text{................................} 3.5$$

Where, $\Delta m$, $\Delta\rho$, $\Delta A$ and $\Delta L$ are the errors in mass, density, area and length.

The calculated porosity measurement is ± 1.65%.

## 3.6. Velocity Uncertainty measurements:

Velocity for both P- and S-wave were estimated by using the same formula as mentioned above in equation 2.5 & 2.6.

The expression used for the calculation of velocities:

$$V = \frac{L}{tm - ts}$$
$$\text{..........................................................................} 3.6$$

Where, V represents the P-and S-wave velocities in m/s, L is the sample length, tm is the measured travel time and ts is the system travel time respectively. Regarding error estimation for velocity measurement and to keep the certain parameters in mind the formula used for equation is:

$$\Delta V = \frac{\delta V}{\delta L}\Delta L + \frac{\delta V}{\delta tm}\Delta tm + \frac{\delta V}{\delta ts}\Delta ts \text{................................................} 3.7$$

Where, $\Delta ts$ and $\Delta tm$ are the error estimation in travel time and $\Delta L$ is the magnitude error in the sample height measurement.

The calculated velocity measurements was ± 55m/sec (3.1%) and 80 m/sec (4.4%).

# Chapter 4: Experimental Results and Analysis

This chapter reviews the experimental results for both the cases (01 & 02). In case#01, the vertical P-wave (Vpz) and the S-wave (Vsz) velocities for pure sand with different percentage of brine are presented here as a function of net vertical stress during loading and unloading cycles in Figure 4.1 to 4.7 in an oedometer setup. The horizontal stress in an oedometer setup could not measure. The changes in vertical P wave velocity with respect to stress are then measured. The vertical S wave propogates along the applied stress direction and its particle displacement occur normal to the direction of propagation. For all of the tests Ottawa (GS# 30-70) was used but the brine percentage was different as shown in Table 3.1 to see the possible effect on velocities because of brine. The behavior of velocities with respect to the stress are presented here graphically for both loading and unloading cycles for each of the case individually to make it easy to understand for the reader. However Vp/Vs change with percentage of brine is also presented to see the velocity effect due to brine in Figure 4.7.

Similarly for case#02 the P-wave and S-wave velocities are presented graphically as a function of net vertical stress for dry and saturated samples in both loading and unloading cycles in Figure 4.10 to 4.19 respectively. However for the case#02 sample description is shown in the Table 3.2. There is also comparison of the (Vp/Vs) change in both dry and saturated samples for loading and unloading cycles are also presented graphically as a function of net vertical stress in Figure 4.20. Later there is also graphical presentation of strain sensitivity and change in porosity against net vertical stress for case#01 in Figure 4.8 & 4.9 and for the case#02 in Figure 4.21 & 4.22 respectively.

Table 4.1 to 4.7 represents the experimental results for both the cases (01&02) which include all the test for loading and unloading cycles. However data presented here for the first case (01) is only for loading, unloading data is presented in appendix B.

**Table 4. 1 Experimental results for Ottawa sand (0 wt %) salanity**

| 0 wt % Loading | | | | |
|---|---|---|---|---|
| Net Vertical Stress (Mpa) | Vpz (m/sec) | Vsz (m/sec) | Strain ( Av mStrain) | Porosity |
| 1.40 | 588 | 381 | 4.56901 | 0.43 |
| 2.08 | 688 | 383 | 9.44770 | 0.42 |
| 2.76 | 781 | 455 | 12.72111 | 0.42 |
| 3.44 | 836 | 456 | 16.07784 | 0.42 |
| 4.12 | 896 | 496 | 19.13478 | 0.42 |
| 4.79 | 944 | 497 | 22.34038 | 0.42 |
| 5.47 | 976 | 518 | 25.10899 | 0.42 |
| 6.14 | 1011 | 520 | 29.66530 | 0.42 |
| 6.81 | 1044 | 536 | 32.63320 | 0.42 |
| 7.48 | 1083 | 538 | 36.61730 | 0.42 |
| 8.15 | 1104 | 554 | | 0.42 |
| 8.66 | 1120 | 556 | | 0.42 |
| 9.19 | 1131 | 572 | | |

| 9.83 | 1174 | 575 | | |
|------|------|-----|---|---|
| 10.59 | 1173 | 595 | | |
| 10.98 | 1173 | 596 | | |
| 11.10 | 1182 | 610 | | |
| 11.10 | 1171 | 612 | | |

**Table 4. 2 Experimental results for Ottawa sand (3.5 wt %) salanity**

| 3.5 wt % Loading | | | | |
|------------------|---|---|---|---|
| **Net Vertical Stress (Mpa)** | **Vpz (m/sec)** | **Vsz (m/sec)** | **Strain ( Av mStrain)** | **Porosity** |
| 1.40 | 1966 | 211 | 17.06734 | 0.46 |
| 2.08 | 1976 | 235 | 22.64504 | 0.44 |
| 2.76 | 1982 | 251 | 28.47773 | 0.44 |
| 3.44 | 1987 | 264 | 31.01346 | 0.44 |
| 4.12 | 1998 | 274 | 33.12102 | 0.44 |
| 4.79 | 2003 | 281 | 34.79821 | 0.44 |
| 5.47 | 2009 | 287 | 36.51660 | 0.43 |
| 6.14 | 2017 | 293 | 38.05110 | 0.43 |
| 6.81 | 2023 | 298 | 39.20894 | 0.43 |
| 7.48 | 2031 | 303 | 40.87094 | 0.43 |
| 8.15 | 2042 | 306 | 42.10488 | 0.43 |
| 8.66 | 2044 | 309 | | |
| 9.19 | 2047 | 312 | | |
| 9.83 | 2056 | 315 | | |
| 10.59 | 2060 | 317 | | |
| 10.98 | 2059 | 318 | | |
| 11.10 | 2062 | 318 | | |

**Table 4. 3 Experimental results for Ottawa sand (0 wt %) salanity**

| 7 wt % Unloading | | | | |
|---|---|---|---|---|
| **Net Vertical Stress (Mpa)** | **Vpz (m/sec)** | **Vsz (m/sec)** | **Strain ( Av mStrain)** | **Porosity** |
| 10.706 | 2423 | 697 | 29.63181 | 0.42 |
| 10.244 | 2415 | 691 | 29.26167 | 0.41 |
| 9.749 | 2413 | 687 | 28.75879 | 0.41 |
| 9.237 | 2402 | 683 | 28.25580 | 0.41 |
| 8.769 | 2393 | 677 | 27.68087 | 0.41 |
| 8.200 | 2382 | 669 | 26.91318 | 0.41 |
| 7.520 | 2358 | 661 | 25.94600 | 0.41 |
| 6.821 | 2328 | 651 | 24.64576 | 0.41 |
| 6.115 | 2307 | 638 | 22.63472 | 0.41 |
| 5.407 | 2297 | 623 | 18.26423 | 0.41 |
| 4.698 | | 603 | | 0.41 |
| 3.629 | | 577 | | |
| 2.916 | | 541 | | |
| 2.203 | | 481 | | |
| 1.845 | | 443 | | |
| 1.131 | | | | |
| 0.774 | | | | |

**Table 4. 4 Experimental results for Dry & Saturated Clos (GS#450-550)**

| Cols (GS#450-550) Dry & Saturated Loading & Unloading | | | | | |
|---|---|---|---|---|---|
| | Net vertical stress (Mpa) | Vpz (m/sec) | Vsz (m/sec) | Strain (Av mStrain) | Porosity |
| **Dry** | 0.48 | 780 | 450 | 4.30913 | 0.47 |
| | 1.40 | 733 | 457 | 9.16432 | 0.45 |
| | 2.43 | 831 | 456 | 12.26773 | 0.45 |
| | 3.46 | 888 | 488 | 14.91272 | 0.45 |
| | 4.48 | 936 | 515 | 17.36354 | 0.45 |
| | 5.50 | 979 | 539 | 19.73173 | 0.45 |
| | 6.51 | 1014 | 560 | 22.00208 | 0.45 |
| | 7.52 | 1046 | 579 | 24.30824 | 0.45 |
| | 8.45 | 1079 | 594 | 26.51411 | 0.44 |
| | 9.21 | 1102 | 610 | 28.35212 | 0.44 |
| | 10.61 | 1137 | 631 | 31.70467 | 0.44 |
| **1st Loading finished** | 11.32 | 1158 | 635 | 34.50051 | 0.44 |
| | 10.54 | 1161 | 632 | 35.32620 | 0.44 |
| | 9.23 | 1150 | 626 | 35.09246 | 0.44 |
| | 8.56 | 1140 | 620 | 34.92375 | 0.44 |
| | 7.55 | 1127 | 612 | 34.64171 | 0.44 |
| | 6.49 | 1111 | 602 | 34.28407 | 0.44 |
| | 5.42 | 1088 | 588 | 33.83233 | 0.44 |
| | 4.36 | 1060 | 574 | 33.27423 | 0.44 |
| | 3.64 | 1035 | 556 | 32.81301 | 0.44 |
| | 2.56 | 985 | 521 | 31.91901 | 0.44 |
| | 1.48 | 905 | 459 | 30.60950 | 0.44 |
| **1st Unloading finished** | 0.47 | 752 | 389 | 25.52055 | 0.44 |
| | 1.42 | 772 | 455 | 28.74216 | 0.44 |
| | 2.45 | 882 | 501 | 30.38217 | 0.44 |
| | 3.47 | 971 | 527 | 31.68900 | 0.44 |
| | 4.49 | 1001 | 551 | 32.81476 | 0.44 |
| | 5.51 | 1040 | 572 | 33.82641 | 0.44 |
| | 6.52 | 1072 | 589 | 34.74685 | 0.44 |
| | 7.53 | 1102 | 605 | 35.62858 | 0.44 |
| | 8.46 | 1127 | 617 | 36.54534 | 0.44 |
| | 9.25 | 1147 | 630 | 37.33949 | 0.44 |
| | 10.22 | 1161 | 640 | 38.29176 | 0.44 |
| | 10.69 | 1189 | 649 | 38.80458 | 0.43 |
| **2nd Loading finished** | 11.16 | 1192 | 645 | 39.34596 | 0.43 |
| | 9.28 | 1180 | 640 | 39.77269 | 0.43 |
| | 8.57 | 1150 | 630 | 39.59076 | 0.43 |

| | | | | |
|---|---|---|---|---|
| | 7.55 | 1160 | 628 | 39.27619 | 0.43 |
| | 6.49 | 1143 | 618 | 38.90169 | 0.43 |
| | 5.43 | 1121 | 606 | 38.45158 | 0.44 |
| | 4.36 | 1095 | 588 | 37.91077 | 0.44 |
| | 3.64 | 1070 | 574 | 37.46795 | 0.44 |
| | 2.57 | 1022 | 542 | 36.60857 | 0.44 |
| **2nd Unloading finished** | 1.49 | 944 | 484 | 35.37227 | 0.44 |
| **Saturation Started** | 2.57 | 1871 | 482 | 34.35497 | 0.44 |
| | 3.47 | 1884 | 503 | 35.20301 | 0.44 |
| | 4.49 | 1899 | 525 | 36.07550 | 0.44 |
| | 5.51 | 1911 | 544 | 36.85469 | 0.44 |
| | 6.52 | 1922 | 560 | 37.61011 | 0.44 |
| | 7.53 | 1930 | 575 | 38.32803 | 0.43 |
| | 8.47 | 1940 | 587 | 38.97289 | 0.43 |
| | 9.24 | 1943 | 596 | 39.50974 | 0.43 |
| **3rd Loading finished** | 10.55 | 1957 | 612 | 40.70555 | 0.43 |
| | 9.24 | 1961 | 618 | 40.81143 | 0.43 |
| | 8.54 | 1956 | 614 | 40.64239 | 0.43 |
| | 7.55 | 1952 | 610 | 40.33117 | 0.43 |
| | 6.50 | 1951 | 605 | 39.94723 | 0.43 |
| | 5.43 | 1942 | 597 | 39.45129 | 0.43 |
| | 4.36 | 1935 | 588 | 38.84619 | 0.43 |
| | 3.65 | 1927 | 580 | 38.32512 | 0.43 |
| | 2.69 | 1920 | 566 | 37.30212 | 0.43 |
| **3rd Unloading finished** | 1.51 | 1901 | 547 | 35.07410 | 0.43 |

4.5

**Table 4. 5 Experimental results for Dry & Saturated Clos (GS#30)**

| Cols (GS#30) Dry & Saturated Loading & Unloading | | | | | |
|---|---|---|---|---|---|
| | Net vertical stress (Mpa) | Vpz (m/sec) | Vsz (m/sec) | Strain (Av mStrain) | Porosity |
| **Dry** | 0.48 | 696 | 540 | 4.30913 | 0.41 |
| | 1.40 | 694 | 579 | 9.16432 | 0.41 |
| | 2.43 | 766 | 682 | 12.26773 | 0.41 |
| | 3.46 | 812 | 759 | 14.91272 | 0.41 |
| | 4.48 | 859 | 812 | 17.36354 | 0.41 |
| | 5.50 | 920 | 859 | 19.73173 | 0.41 |
| | 6.51 | 927 | 899 | 22.00208 | 0.40 |
| | 7.52 | 977 | 936 | 24.30824 | 0.40 |
| | 8.45 | 988 | 967 | 26.51411 | 0.40 |
| | 9.21 | 999 | 991 | 28.35212 | 0.40 |
| | 10.61 | 1044 | 1033 | 31.70467 | 0.40 |
| **1st Loading finished** | 11.32 | 1060 | 1061 | 34.50051 | 0.40 |
| | 10.54 | 1060 | 1059 | 35.32620 | 0.40 |
| | 9.23 | 1055 | 1052 | 35.09246 | 0.40 |
| | 8.56 | 1042 | 1041 | 34.92375 | 0.40 |
| | 7.55 | 1030 | 1029 | 34.64171 | 0.40 |
| | 6.49 | 1015 | 1010 | 34.28407 | 0.40 |
| | 5.42 | 998 | 987 | 33.83233 | 0.40 |
| | 4.36 | 964 | 958 | 33.27423 | 0.40 |
| | 3.64 | 942 | 935 | 32.81301 | 0.40 |
| | 2.56 | 895 | 885 | 31.91901 | 0.40 |
| | 1.48 | 822 | 811 | 30.60950 | 0.40 |
| **1st Unloading finished** | 0.47 | 587 | 637 | 25.52055 | 0.40 |
| | 1.42 | 634 | 578 | 28.74216 | 0.40 |
| | 2.45 | 807 | 665 | 30.38217 | 0.40 |
| | 3.47 | 856 | 770 | 31.68900 | 0.40 |
| | 4.49 | 902 | 831 | 32.81476 | 0.40 |
| | 5.51 | 940 | 878 | 33.82641 | 0.40 |
| | 6.52 | 967 | 916 | 34.74685 | 0.40 |
| | 7.53 | 993 | 949 | 35.62858 | 0.40 |
| | 8.46 | 1016 | 976 | 36.54534 | 0.40 |
| | 9.25 | 1035 | 1002 | 37.33949 | 0.39 |
| | 10.22 | 1050 | 1015 | 38.29176 | 0.39 |
| | 10.69 | 1081 | 1061 | 38.80458 | 0.39 |
| **2nd Loading finished** | 11.16 | 1079 | 1083 | 39.34596 | 0.39 |
| | 9.28 | 1071 | 1076 | 39.77269 | 0.39 |
| | 8.57 | 1060 | 1060 | 39.59076 | 0.39 |
| | 7.55 | 1052 | 1054 | 39.27619 | 0.39 |
| | 6.49 | 1032 | 1040 | 38.90169 | 0.39 |
| | 5.43 | 1013 | 1018 | 38.45158 | 0.39 |

| | | | | | |
|---|---|---|---|---|---|
| | 4.36 | 984 | 993 | 37.91077 | 0.39 |
| | 3.64 | 960 | 973 | 37.46795 | 0.40 |
| | 2.57 | 911 | 935 | 36.60857 | 0.40 |
| **2nd Unloading finished** | 1.49 | 843 | 850 | 35.37227 | 0.40 |
| <span style="color:red">**Saturation Started**</span> | <span style="color:red">2.57</span> | <span style="color:red">1797</span> | <span style="color:red">884</span> | <span style="color:red">34.35497</span> | <span style="color:red">0.39</span> |
| | 3.47 | 1812 | 823 | 35.20301 | 0.39 |
| | 4.49 | 1822 | 691 | 36.07550 | 0.39 |
| | 5.51 | 1835 | 867 | 36.85469 | 0.39 |
| | 6.52 | 1844 | 837 | 37.61011 | 0.39 |
| | 7.53 | 1852 | 846 | 38.32803 | 0.39 |
| | 8.47 | 1860 | 852 | 38.97289 | 0.39 |
| | 9.24 | 1865 | 859 | 39.50974 | 0.39 |
| **3rd Loading finished** | 10.55 | 1878 | 860 | 40.70555 | 0.39 |
| | 9.24 | 1879 | 857 | 40.81143 | 0.39 |
| | 8.54 | 1875 | 851 | 40.64239 | 0.39 |
| | 7.55 | 1872 | 844 | 40.33117 | 0.39 |
| | 6.50 | 1865 | 849 | 39.94723 | 0.40 |
| | 5.43 | 1857 | 851 | 39.45129 | 0.42 |
| | 4.36 | 1851 | 853 | 38.84619 | 0.43 |
| | 3.65 | 1845 | 853 | 38.32512 | 0.43 |
| | 2.69 | 1832 | 853 | 37.30212 | 0.43 |
| **3rd Unloading finished** | 1.51 | 1789 | 855 | 35.07410 | 0.43 |

**Table 4. 6 Experimental results for Dry & Saturated OT (GS#30-70)**

| OT (GS#30-70) Dry &saturated Loading & Unloading | | | | | |
|---|---|---|---|---|---|
| | **Net vertical stress (Mpa)** | **Vpz (m/sec)** | **Vsz (m/sec)** | **Strain (Av mStrain)** | **Porosity** |
| **Dry** | 0.48 | 681 | 306 | 10.01000 | 0.38 |
| | 1.40 | 669 | 305 | 10.24384 | 0.38 |
| | 2.43 | 795 | 314 | 13.28969 | 0.37 |
| | 3.46 | 869 | 339 | 15.56182 | 0.37 |
| | 4.48 | 908 | 350 | 15.56182 | 0.37 |
| | 5.50 | 953 | 365 | 16.77633 | 0.37 |
| | 6.51 | 992 | 376 | 18.35352 | 0.37 |
| | 7.52 | 1025 | 386 | 19.81627 | 0.37 |
| | 8.45 | 1052 | 394 | 21.10110 | 0.37 |
| | 9.21 | 1077 | 401 | 22.31932 | 0.37 |
| | 10.61 | 1094 | 406 | 23.18679 | 0.37 |
| **1st Loading finished** | 11.32 | 1129 | 415 | 24.33556 | 0.37 |
| | 10.54 | 1140 | 419 | 25.81103 | 0.37 |
| | 9.23 | 1141 | 419 | 22.22889 | 0.37 |

| | | | | |
|---|---|---|---|---|
| | 8.56 | 1132 | 417 | 25.54033 | 0.37 |
| | 7.55 | 1128 | 416 | 25.54033 | 0.37 |
| | 6.49 | 1120 | 414 | 25.14543 | 0.37 |
| | 5.42 | 1109 | 411 | 24.82541 | 0.37 |
| | 4.36 | 1098 | 409 | 24.20873 | 0.37 |
| | 3.64 | 1079 | 404 | 23.46335 | 0.37 |
| | 2.56 | 1058 | 398 | 22.90534 | 0.37 |
| | 1.48 | 1039 | 393 | 21.75883 | 0.37 |
| **1st Unloading finished** | 0.47 | 974 | 374 | 20.12313 | 0.37 |
| | 1.42 | 821 | 325 | 16.50472 | 0.37 |
| | 2.45 | 902 | 321 | 18.77658 | 0.37 |
| | 3.47 | 831 | 321 | 20.44559 | 0.37 |
| | 4.49 | 884 | 339 | 21.36854 | 0.37 |
| | 5.51 | 949 | 360 | 22.59265 | 0.37 |
| | 6.52 | 985 | 371 | 24.90642 | 0.37 |
| | 7.53 | 1017 | 381 | 24.58131 | 0.37 |
| | 8.46 | 1045 | 390 | 25.46485 | 0.37 |
| | 9.25 | 1072 | 397 | 26.35521 | 0.37 |
| | 10.22 | 1093 | 404 | 27.29566 | 0.36 |
| | 10.69 | 1118 | 411 | 28.45999 | 0.36 |
| **2nd Loading finished** | 11.16 | 1155 | 421 | 28.53947 | 0.36 |
| | 9.28 | 1157 | 422 | 28.20871 | 0.36 |
| | 8.57 | 1150 | 420 | 27.86535 | 0.36 |
| | 7.55 | 1145 | 419 | 27.55392 | 0.36 |
| | 6.49 | 1137 | 417 | 26.99162 | 0.36 |
| | 5.43 | 1124 | 414 | 26.33708 | 0.37 |
| | 4.36 | 1114 | 412 | 25.81497 | 0.37 |
| | 3.64 | 1097 | 408 | 24.78126 | 0.37 |
| | 2.57 | 1075 | 402 | 23.28985 | 0.37 |
| **2nd Unloading finished** | 1.49 | 1049 | 744 | 21.21243 | 0.37 |
| **Saturation Started** | 2.57 | 992 | 745 | 19.73644 | 0.37 |
| | 3.47 | 1800 | 758 | 21.23462 | 0.37 |
| | 4.49 | 1808 | 768 | 22.24141 | 0.37 |
| | 5.51 | 1829 | 772 | 23.70660 | 0.37 |
| | 6.52 | 1847 | 774 | 25.14746 | 0.37 |
| | 7.53 | 1853 | 776 | 27.14986 | 0.37 |
| | 8.47 | 1868 | 779 | 26.74795 | 0.37 |
| | 9.24 | 1877 | 782 | 26.95409 | 0.36 |
| **3rd Loading finished** | 10.55 | 1883 | 782 | 29.13272 | 0.37 |
| | 9.24 | 1893 | 784 | 29.65325 | 0.36 |

| | 8.54 | 1907 | 787 | 29.74338 | 0.36 |
|---|---|---|---|---|---|
| | 7.55 | 1908 | 787 | 29.38157 | 0.36 |
| | 6.50 | 1903 | 787 | 29.03279 | 0.36 |
| | 5.43 | 1905 | 787 | 28.70993 | 0.36 |
| | 4.36 | 1898 | 786 | 28.12369 | 0.36 |
| | 3.65 | 1891 | 786 | 27.69159 | 0.36 |
| | 2.69 | 1892 | 786 | 25.73326 | 0.36 |
| **3rd Unloading finished** | 1.51 | 1883 | 785 | 24.33779 | 0.36 |

**Table 4. 7 Experimental results for Dry & Saturated OT (GS#+450)**

| OT (GS#+450) Dry & Saturated Loading Unloading | | | | | |
|---|---|---|---|---|---|
| | Net vertical stress (Mpa) | Vpz (m/sec) | Vsz (m/sec) | Strain (Av mStrain) | Porosity |
| **Dry** | 0.48 | 740 | 489 | 85.00000 | 0.41 |
| | 1.40 | 811 | 413 | 86.36058 | 0.38 |
| | 2.43 | 906 | 461 | 88.72749 | 0.38 |
| | 3.46 | 969 | 499 | 90.53311 | 0.38 |
| | 4.48 | 1020 | 528 | 91.00000 | 0.38 |
| | 5.50 | 1062 | 553 | 92.00000 | 0.38 |
| | 6.51 | 1085 | 567 | 93.91181 | 0.38 |
| | 7.52 | 1120 | 587 | 94.91419 | 0.37 |
| | 8.45 | 1156 | 609 | 96.08290 | 0.37 |
| | 9.21 | 1176 | 621 | 96.73429 | 0.37 |
| | 10.61 | 1195 | 633 | 97.36536 | 0.37 |
| **1st Loading finished** | 11.32 | 1221 | 648 | 98.27372 | 0.37 |
| | 10.54 | 1221 | 649 | 98.38836 | 0.37 |
| | 9.23 | 1210 | 644 | 98.12583 | 0.37 |
| | 8.56 | 1200 | 637 | 97.80835 | 0.37 |
| | 7.55 | 1186 | 630 | 97.41494 | 0.37 |
| | 6.49 | 1175 | 624 | 97.12228 | 0.37 |
| | 5.42 | 1156 | 613 | 96.56725 | 0.37 |
| | 4.36 | 1131 | 600 | 95.89334 | 0.37 |
| | 3.64 | 1096 | 579 | 94.94901 | 0.37 |
| | 2.56 | 1043 | 548 | 93.62150 | 0.38 |
| | 1.48 | 986 | 515 | 92.25395 | 0.38 |
| **1st Unloading finished** | 0.47 | 909 | 675 | 87.94175 | 0.38 |
| | 1.42 | 994 | 466 | 90.35453 | 0.38 |
| | 2.45 | 1044 | 507 | 92.22693 | 0.38 |
| | 3.47 | 1085 | 538 | 93.64117 | 0.38 |

| | | | | |
|---|---|---|---|---|
| | 4.49 | 1119 | 562 | 94.77056 | 0.38 |
| | 5.51 | 1149 | 583 | 95.75849 | 0.37 |
| | 6.52 | 1165 | 595 | 96.34241 | 0.37 |
| | 7.53 | 1187 | 611 | 97.13517 | 0.37 |
| | 8.46 | 1210 | 626 | 97.99428 | 0.37 |
| | 9.25 | 1233 | 639 | 98.47803 | 0.37 |
| | 10.22 | 1247 | 651 | 99.13376 | 0.37 |
| | 10.69 | 1245 | 661 | 99.87461 | 0.37 |
| **2nd Loading finished** | 11.16 | 1233 | 658 | 99.93725 | 0.37 |
| | 9.28 | 1225 | 654 | 99.71172 | 0.37 |
| | 8.57 | 1209 | 647 | 99.40071 | 0.37 |
| | 7.55 | 1191 | 639 | 99.02690 | 0.37 |
| | 6.49 | 1178 | 633 | 98.73045 | 0.37 |
| | 5.43 | 1152 | 621 | 98.20385 | 0.37 |
| | 4.36 | 1118 | 606 | 96.64734 | 0.37 |
| | 3.64 | 1057 | 582 | 95.39045 | 0.37 |
| | 2.57 | 1050 | 545 | 80.31612 | 0.37 |
| **2nd Unloading finished** | 1.49 | 1960 | 511 | 54.69660 | 0.40 |
| **Saturation Started** | 2.57 | 1969 | 513 | 56.20608 | 0.39 |
| | 3.47 | 1990 | 528 | 57.39700 | 0.39 |
| | 4.49 | 2009 | 545 | 58.96817 | 0.39 |
| | 5.51 | 2023 | 552 | 59.86370 | 0.39 |
| | 6.52 | 2040 | 561 | 60.77327 | 0.39 |
| | 7.53 | 2052 | 570 | 61.66996 | 0.39 |
| | 8.47 | 2065 | 581 | 62.25423 | 0.39 |
| | 9.24 | 2075 | 594 | 63.26232 | 0.39 |
| **3rd Loading finished** | 10.55 | 2081 | 608 | 64.03244 | 0.39 |
| | 9.24 | 2099 | 630 | 64.10262 | 0.39 |
| | 8.54 | 2105 | 647 | 63.84095 | 0.39 |
| | 7.55 | 2105 | 650 | 63.49570 | 0.39 |
| | 6.50 | 2099 | 645 | 63.05779 | 0.40 |
| | 5.43 | 2097 | 641 | 62.48494 | 0.42 |
| | 4.36 | 2089 | 636 | 61.84670 | 0.43 |
| | 3.65 | 2083 | 628 | 61.28362 | 0.43 |
| | 2.69 | 2074 | 620 | 60.04871 | 0.43 |
| **3rd Unloading finished** | 1.51 | 2067 | 609 | 57.98052 | 0.43 |

# 4.1. Case#01:

## 4.1.1. Effect of brine percentage on velocities against net vertical stress:

The vertical P-wave (Vpz) and the S-wave (Vsz) velocities for the for the Ottawa (OT) pure sand with different percentage of brine are presented here graphically as a function of net vertical stress during loading and unloading cycles in Figure 4.1 to 4.7 to see the clear effect on velocities with change in brine. All the graphical trends shown here must be viewed in the light of velocity uncertainty discussed in chapter three in Section 3.6. All the plots presented here are constructed individually first for the loading and unloading cycles and then combine to make it clear, sensible and easy for the reader.

The main focus of these experiments with different percentage of brine was to see the change in seismic properties of the rocks like velocities (P- and S-wave) with change in fluid concentration (brine). The vertical P- and S- wave velocity in pure Ottawa sand varies with the change in percentage of brine which is not only fluid dependent but pressure, temperature and density has also an impact on these seismic attributes which needs to further analyzed which are discussed in chapter five section 5.2.

In present study the vertical P- and S- wave velocities are plotted against net vertical stress for different concentration are brine is found dependent on the fluid concentration. As Vpz & Vsz for pure OT sand with 0 wt % brine (fresh water) is found much lower than the Vpz & Vsz are in 3.5 & 7 wt % fluid (brine). So the Velocities are found having the direct relationship with the concentration of brine. In figure 4.5 & 4.6 it can be observed clearly an increase in velocities with increase in brine percentage both during loading and unloading cycles which also shows the velocity hysteresis. Similarly in figure 4.7 the vertical P- and S-wae velocity ratio Vpz/Vsz is also presented to illustrate the velocity sensitivity with brine percentage. The Vpz/Vsz seems to be relatively stable in the lower stress level upto about 5 MPa net vertical stress. However the factors which needs to be considered strongly during evaluation for this graphical presentation is error estimation and also this work was individually done without any comparison with previous experimental data as there were no such velocity comparison with brine found on web. A discussed above further evaluation must be done regarding present data presented in this project in order to understand the change in seismic attributes with fluid (brine) concentration change.

**Figure 4. 1  P-wave Velocity Plot   against net vertical stress during loading for different percentage of brine**
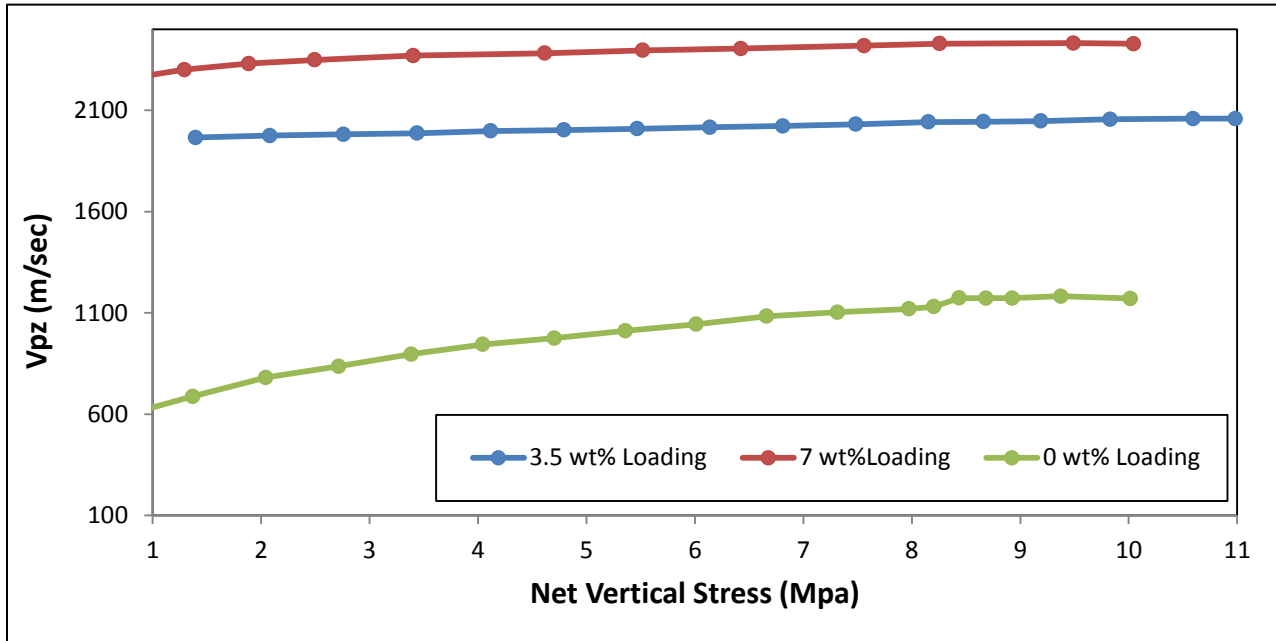


**Figure 4. 2 P-wave velocity plot against net vertical stress during Unloading cycles for different percentage of brine**
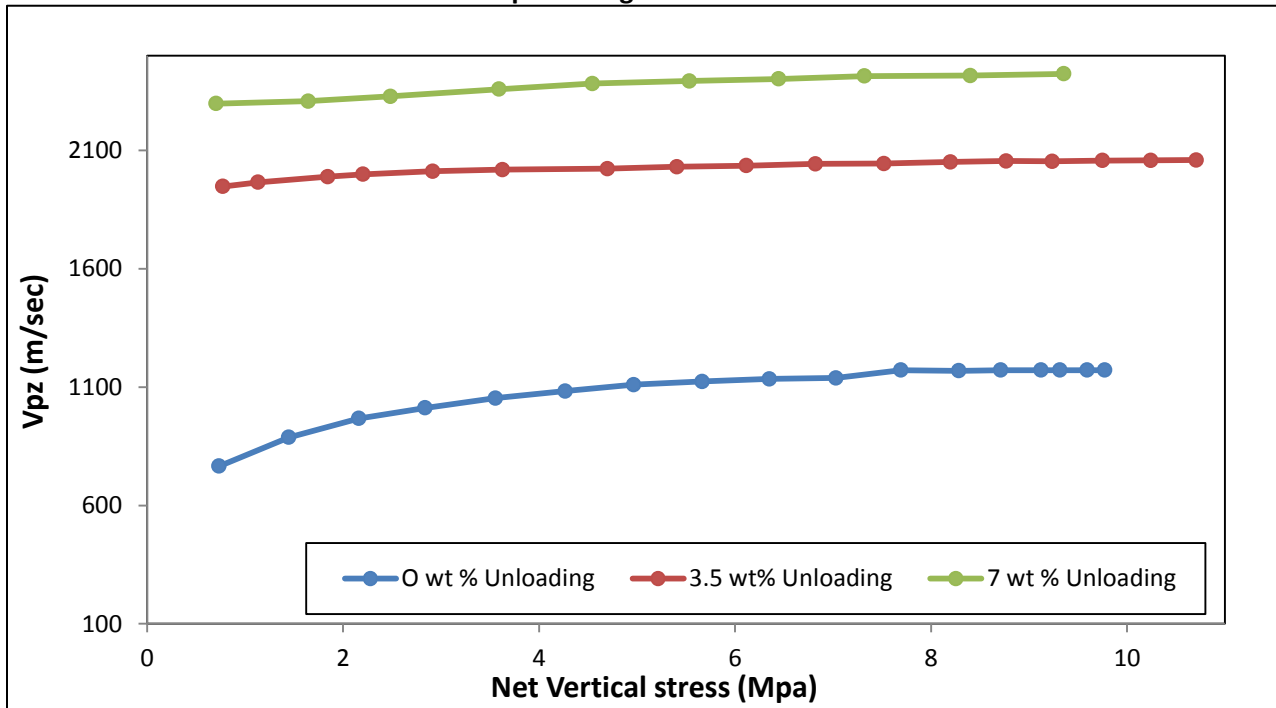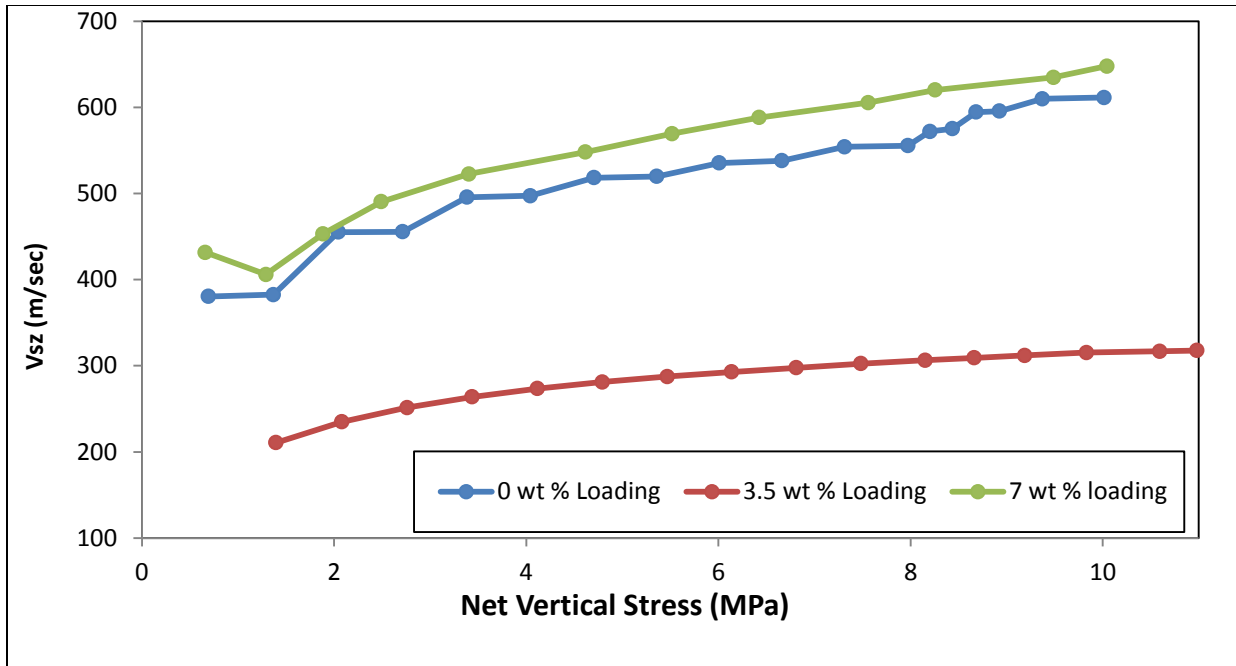
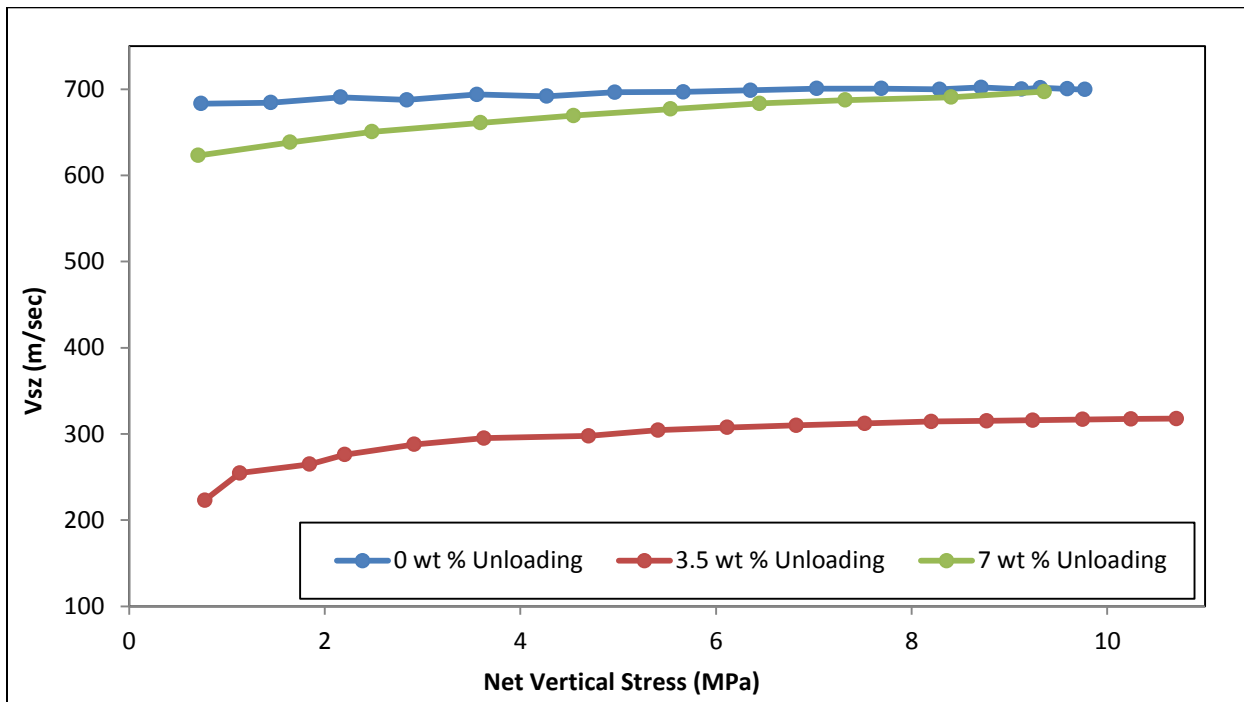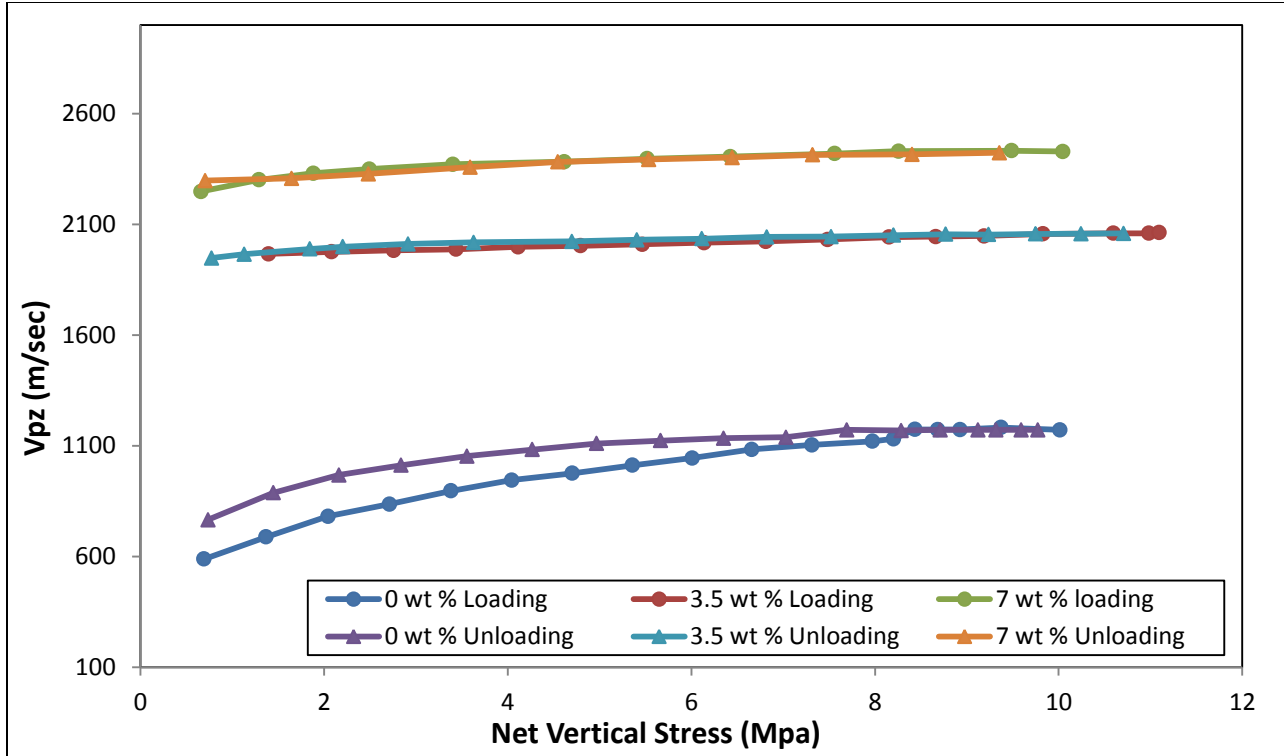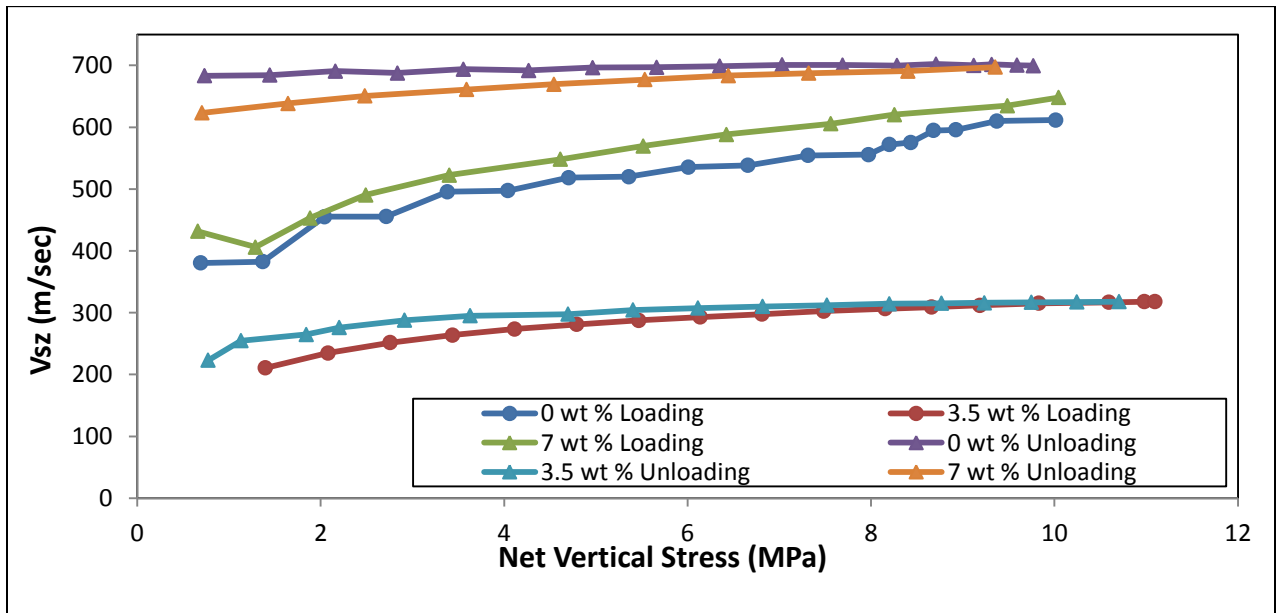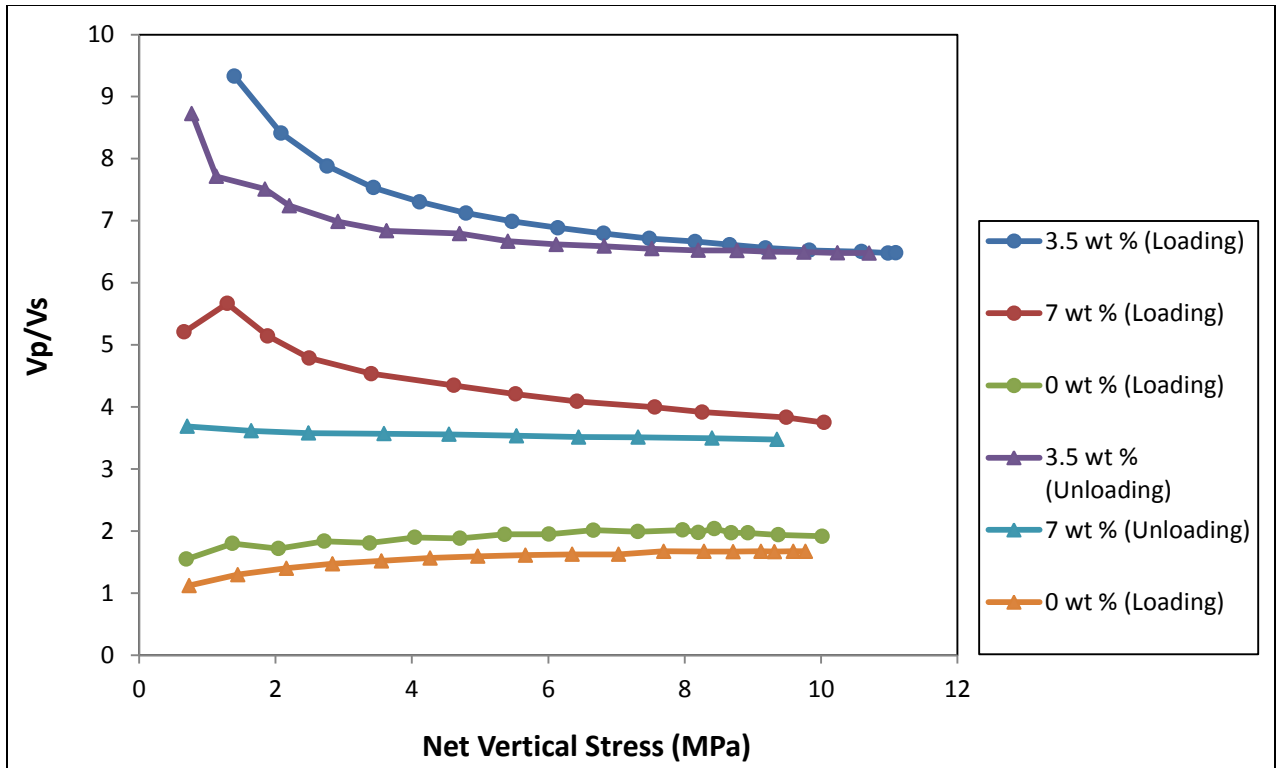**Figure 4. 3  S-wave Velocity Plot  against net vertical stress during loading for different percentage of brine**



**Figure 4. 4 S-wave Velocity plot against net vertical stress during Unloading for different percentage of brine**

**Figure 4. 5 P-wave Velocity plot against net vertical stress during loading and unloading cycles for different percentage of brine**



**Figure 4. 6 S-wave Velocity plot against bet vertical stress during loading and unloading cycles for different percentage of brine**

**Figure 4. 7 Vp/Vs Velocity plot against net vertical stress during loading and unloading for different percentage of brine**

# 4.2. Case#01:

## 4.2.1. Effect of vertical stress on vertical strain:

### Dry and Saturated Ottawa Sand with all the percentage of brine:

The measured strain (mStrain= 1000*strain) are plotted here as a function of net vertical stress in figure 4.8 for both loading and unloading cycles to demonstrate the absolute strain and their hysteresis behavior of all the studied samples.

All the samples show less stress sensitive strain until the about 1.5 net vertical stresses. All the samples were compacted up to 11.0 MPa net vertical stresses. As the sample used for all the tests were same OT sand with different percentage of brine but still the sample with high concentration of brine show high stress sensitivity with strain than the one with 0 wt % of brine. Since the samples were compacted about 11.0 MPa net vertical stresses, it can be termed as consolidated samples; therefore less strain sensitivity would expected as it shown in figure 4.8. All the samples presented here are showing the inelastic behavior because none of the sample returns to their original shape which shows the strain hysteresis. However for this behavior, friction of the piston and wall need to be considered.
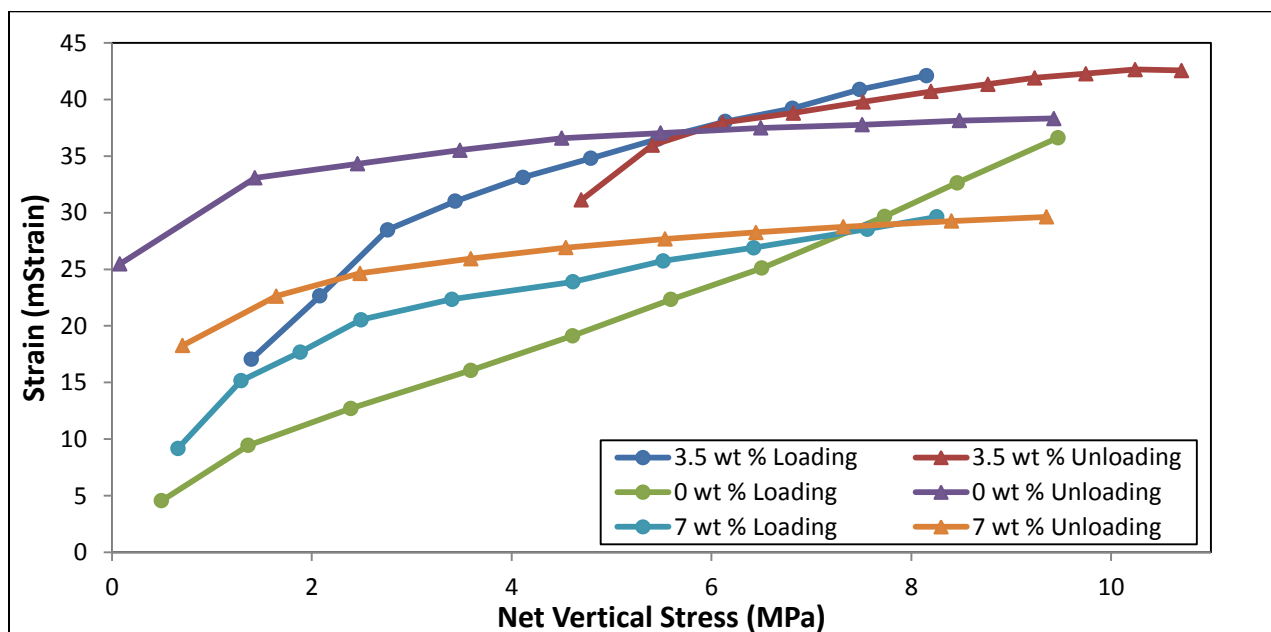


**Figure 4. 8  Stress plot against Strain explaining the strain sensitivity and strain hysteresis during loading and unloading cycles**

# 4.3. Case#01:

## 4.3.1. Effect of vertical stress on porosity:

The reduction of the porosity of the particular lithology especially for sandy lithology is not only dependent on the applied stress but there are also other factors which involves in porosity reduction which are discussed in chapter two Section 2.2.4. Initial porosity for all the samples were measured with the formula mentioned above in chapter 3 section 3.5. However the porosity reduction with stress is illustrated briefly further in section 4.9.1. Figure 4.9 showing the change in porosity with stress which seems to be stable or very low for both loading and unloading cycles.
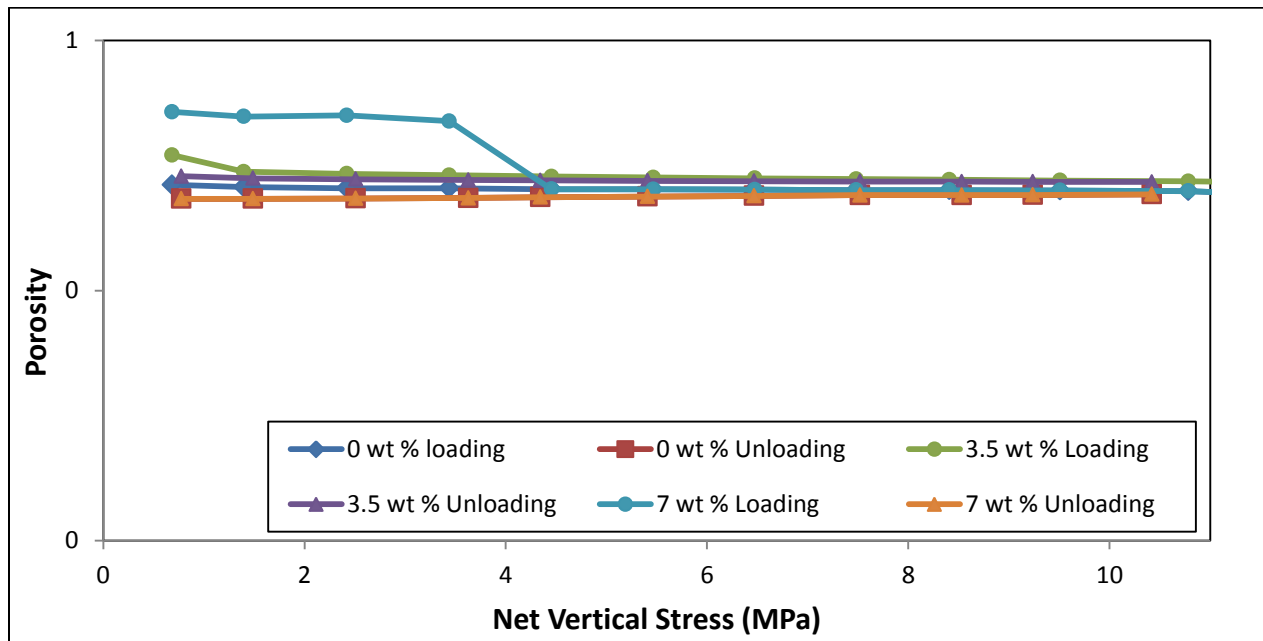


**Figure 4. 9 Showing the porosity change with respect to the vertical stress both in loading and unloading cycles**

# 4.4. Case#02

## 4.4.1. Effect of vertical stress and grain sizes on velocities:

### Dry and Saturated Columbia Sand (GS#450-550):

Figure 4.10 & 4.11 shows the velocity and stress sensitivity of vertical P- and S- wave for both dry and saturated sample during loading and unloading cycles. The effect on vertical stress on Vpz and Vsz presented here showing more stress sensitive which could be possibly because of the development of the grain contact due to net stress. However Vpz found in saturated case is much higher than the dry one which can be a clear indication of fluid effect on velocity. So figure 4.10 show the direct relation between the velocity changes with the fluid substitution. While figure 4.11 shows the change in Vsz which doesn't show quite change for dry and saturated case as S- wave have no effect with th fluid substitution. Moreover effect of net vertical stress on velocity on velocity and velocity hysteresis can also be clearly observed in figure 4.10 which shows the perfect velocity hysteresis. However the behavior of P- and S- wave velocity and there ratio (Vp/Vs) with development of grain contact which can be made by applying vertical stress and with fluid are also presented graphically and explained briefly in section 4.5 to 4.7 and in figures 4.18 to 4.20 for all the samples with different grain sizes.
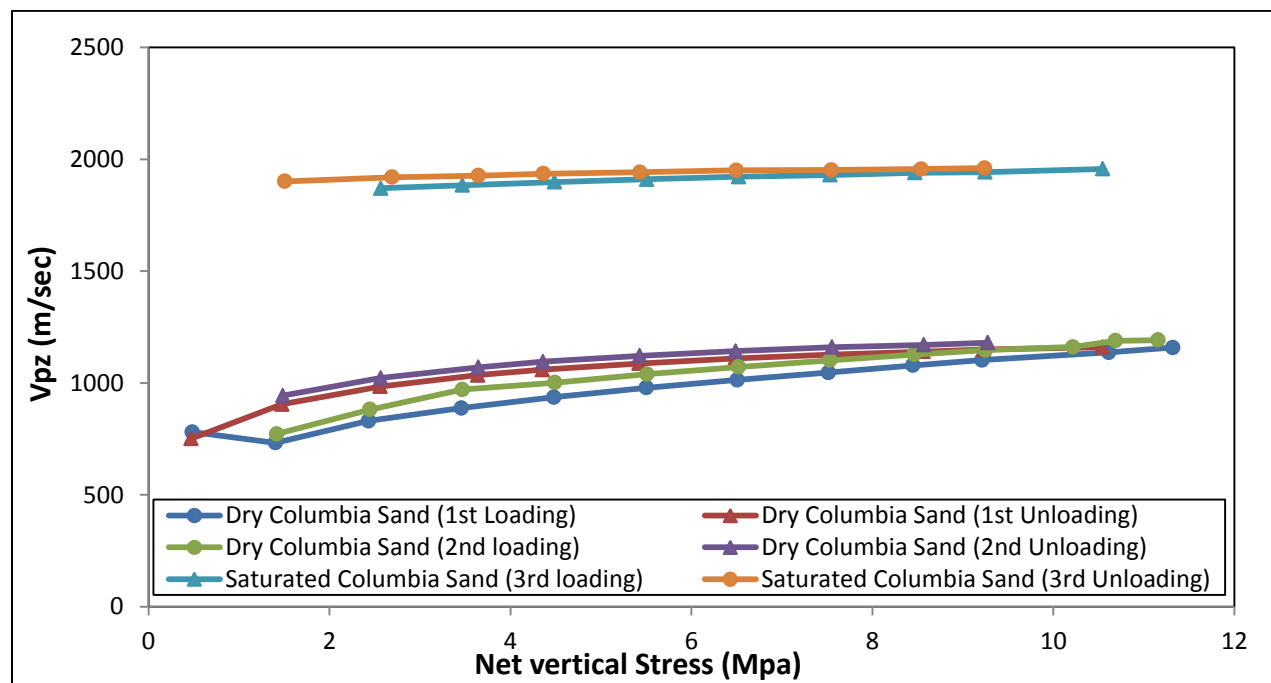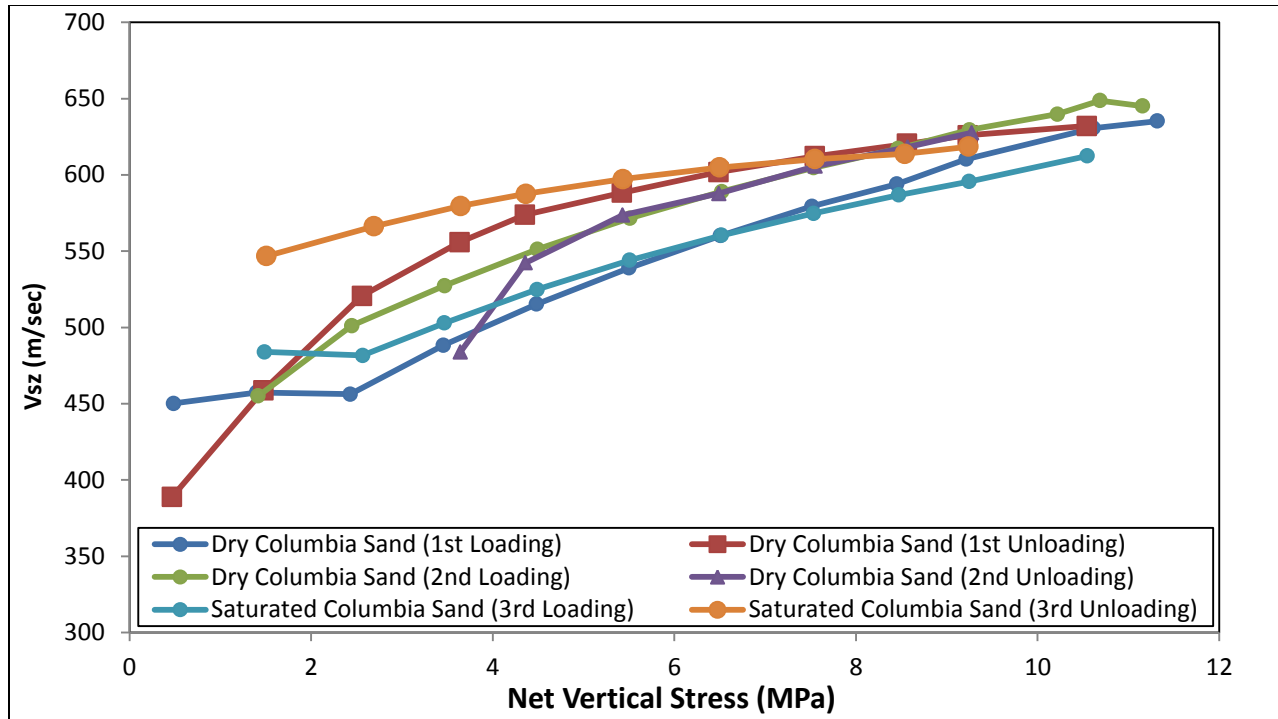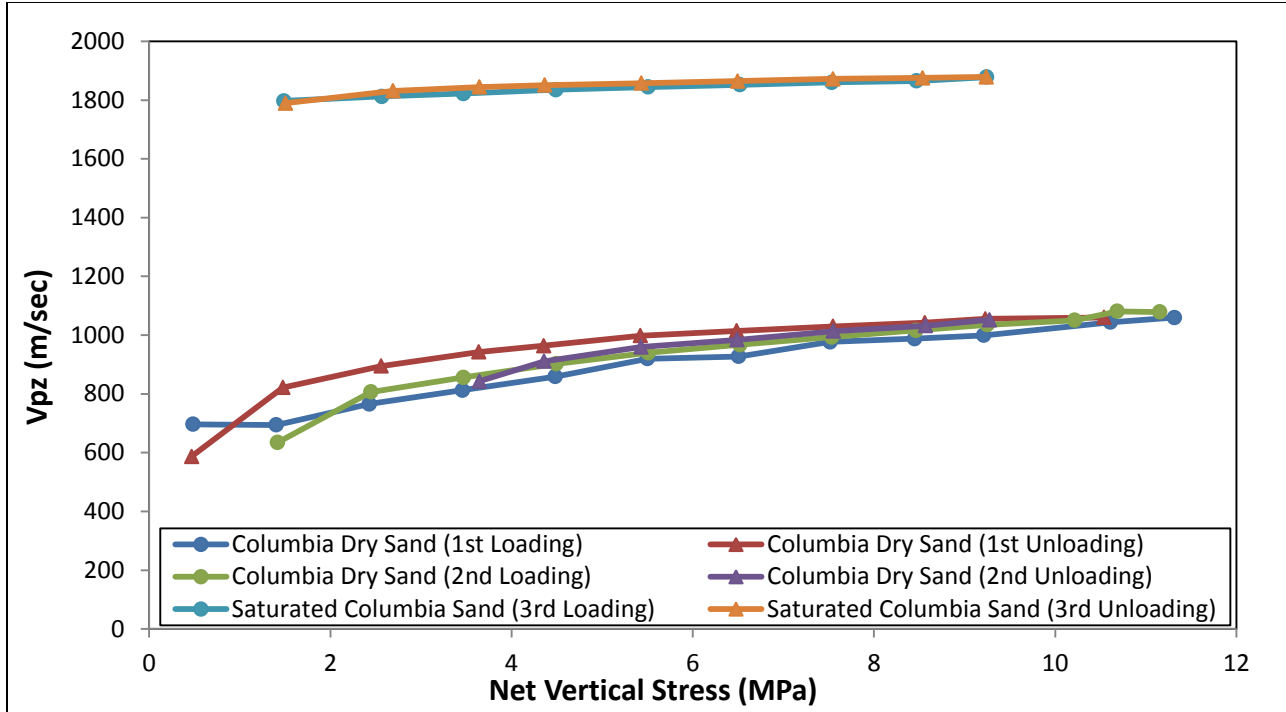


**Figure 4. 10 P-wave velocity plot against net vertical stress during loading and unloading cycles for Cols (GS#450-550)**

**Figure 4. 11 S-wave velocity plot against net vertical stress during loading and unloading cycles for Cols (GS#450-550)**

## Dry and Saturated Columbia Sand (GS#30):

The vertical P- and S- wave velocities are plotted against net vertical stress for dry and saturated case for both loading and unloading cycles in figure 4.12 & 4.13. Fluid effect on Vpz can be observed in figure 4.12 as the Vpz increase with the fluid injection and vice versa. However there is no such clear indication of velocity change with grain sizes have been found as prior to the fluid effect. Vsz in figure 4.13 shows the same trend as shown for the previous case in figure 4.11 with no as such effected with the fluid injection.

**Figure 4. 12 P-wave velocity plot against net vertical stress during loading and unloading cycles for Cols (GS#30)**
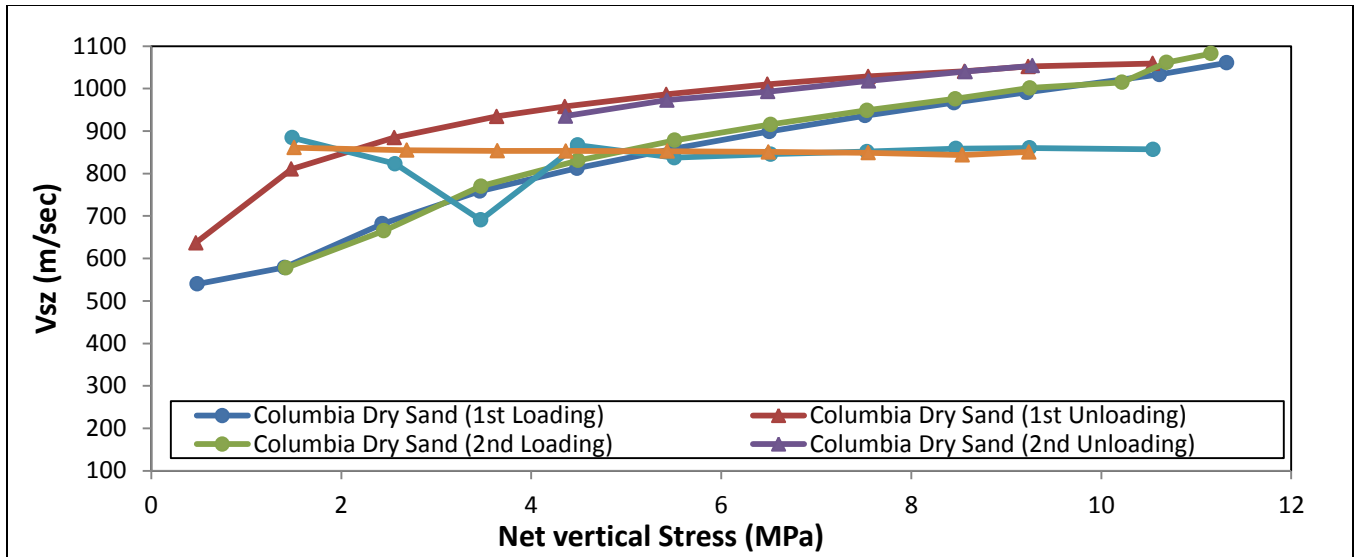
**Figure 4. 13 S-wave velocity plot against net vertical stress during loading and unloading cycles for Cols (GS#30)**

## Dry and Saturated Ottawa Sand (GS# 30-70):

Figure 4.14 & 4.15 presented here graphically as a function of net vertical stress for dry and saturated sample during both loading and unloading cycles. The vertical P-wave velocity in figure 4.14 showing the higher values after fluid injection while in dry case during loading and unloading there is no such big difference in Vpz. While in figure 4.15 showing the higher values for the Vsz after fluid injection which shows the effect on Vsz with fluid which seems to be wrong for that case.
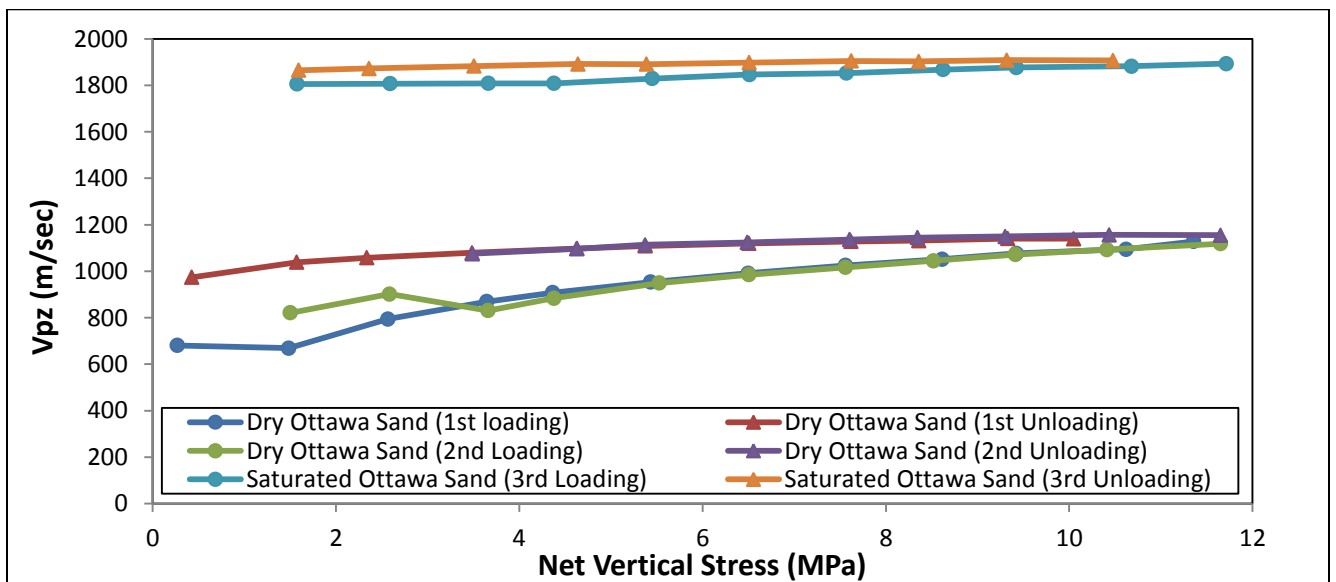


**Figure 4. 14 P-wave velocity plot against net vertical stress during loading and unloading cycles for Cols (GS#30-70)**
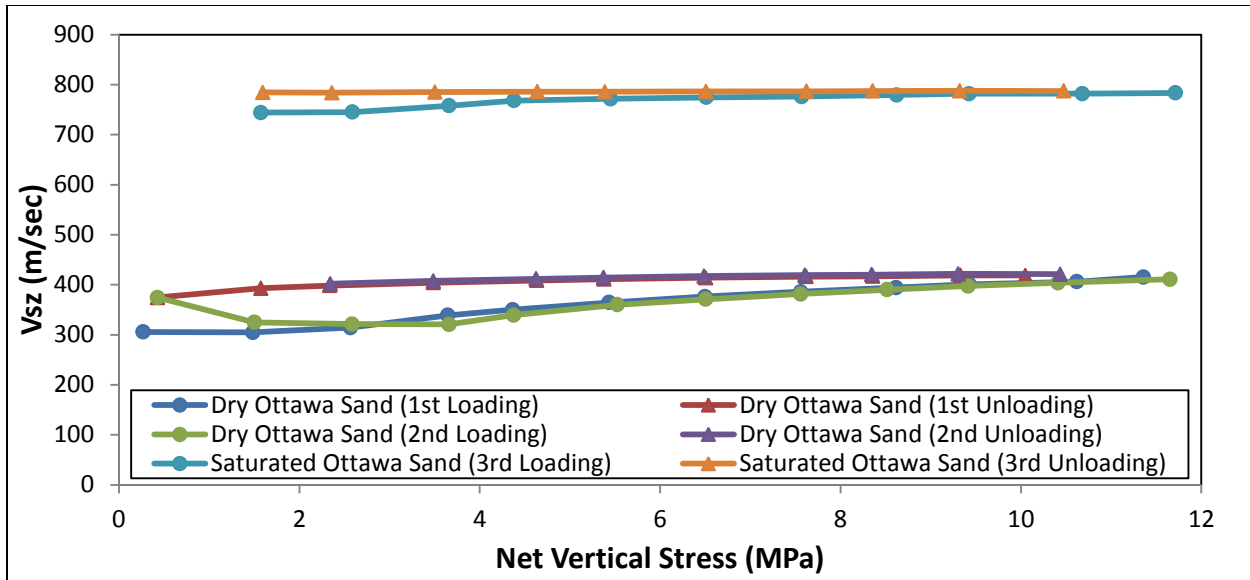
42

**Figure 4. 15 S-wave velocity plot against net vertical stress during loading and unloading cycles for Cols (GS#30-70)**

## Dry and Saturated Ottawa Sand (GS#+450):

Figure 4.16 & 4.17 showing the Vpz and vsz change with respect to the stress and fluid for both loading and unloading cycles. The vertical P- wave velocity in figure 4.16 in dry case seems to be almost same with no such effect with stress but with the fluid injection it's creeping up with clear effect of fluid on Vpz. While in figure 4.17 Vsz shows almost the same behavior in dry and saturated same with clear indication of no fluid effect on S- wave velocity.
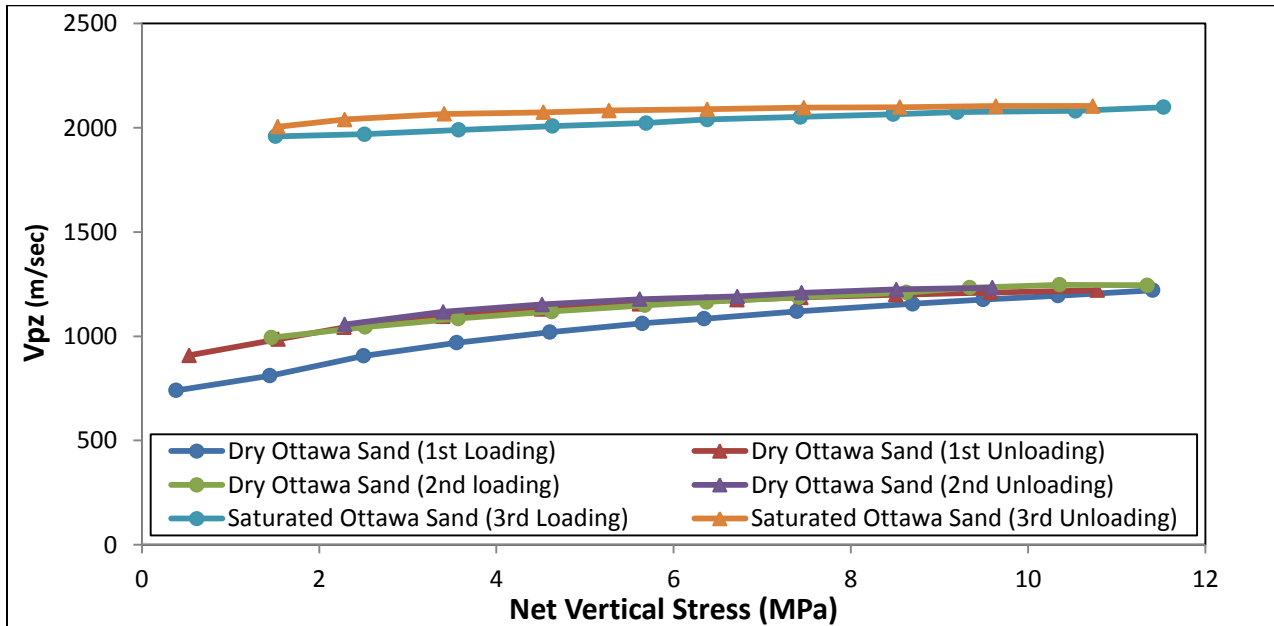


**Figure 4. 16 P-wave velocity plot against net vertical stress during loading and unloading cycles for Cols (GS#+450)**
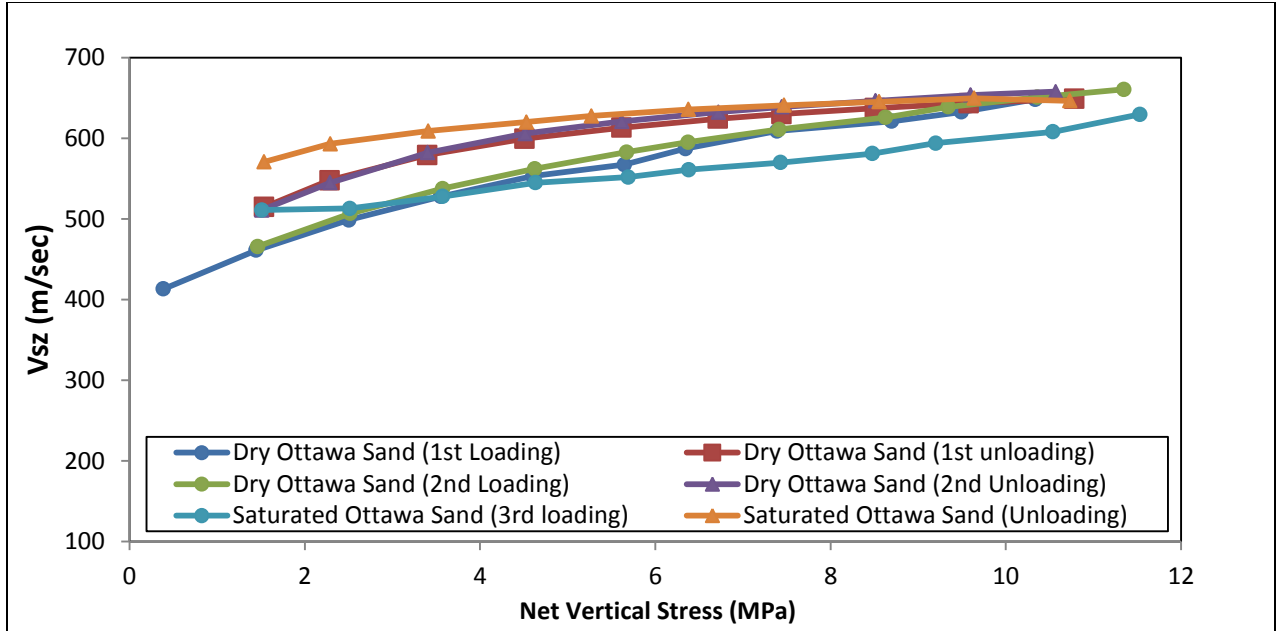
**Figure 4. 17 S-wave velocity plot against net vertical stress during loading and unloading cycles for Cols (GS#+450)**

## 4.5. Dry and Saturated (Vpz) for all the samples during Loading & Unloading cycles:

Domenico (1997) perform an experimental study on unconsolidated brine and gas saturated sand (Ottawa sand) and glass bead which shows nearly identical porosities to calculate the effect of compressive stress and pore fluid properties on elastic properties of unconsolidated sand. He observed that the P- and S- wave velocities for both gas and brine saturated specimen were increased $1/4^{th}$ power of differential pressure. The vertical P- and S- wave velocity in figure 4.18 & 4.19 are plotted against net vertical stress for all the samples in dry and brine saturated sand with different grain sizes during loading and unloading cycles to see the possible effect of fluid and grain contact on velocities. Figure 4.18 shows the Vpz as a function of net vertical stress in all the samples, sample description is given in chapter three section 3.3, Table 3.2. The Vpz shows almost more or less same trend in dry case in both loading and unloading cycles which means that Vpz doesn't have such impact due to different grain sizes. But Vpz has a clear effect due to the fluid substitution which can be clearly observe in figure 4.18. As the velocity values goes higher with substitution of fluid. This increase in velocity is prominent in Vpz as compared to Vsz shown in figure 4.19 where the velocity difference in both dry and saturated doesn't show much difference. This increase in Velocity (Vpz) may be due to the combine effect of increased density of fluid and bulk modulus. However the velocity change due to grain contact doesn't seems to be much higher even on higher stress levels where the development of the grain contact occurred. However the Vpz and Vsz are found more stress sensitive. This might be because of the improvement of grain contact along with the applied stresses as there is no such theoretical references in the literature were found for the velocity behavior with grain sizes.

Figure 4.18 & 4.19 shows the velocities sensitivity with with stress and fluids in all the samples. So it is the evidence in this study that the acoustic velocities changed with change in external stress. Not only that other factors like pore pressure, porosity, clay content, consolidation state, grain size, shape, sorting. Degree of cementation, fluid saturation, fluid type, temperature, digenesis, presence of cracks etc, can have an effect of acoustic properties of the rocks. As it is very difficult to achieve the subsurface conditions in the laboratory but still by considering the effect of factors discussed above one can estimate the velocity and can resemble that with subsurface in some extent.
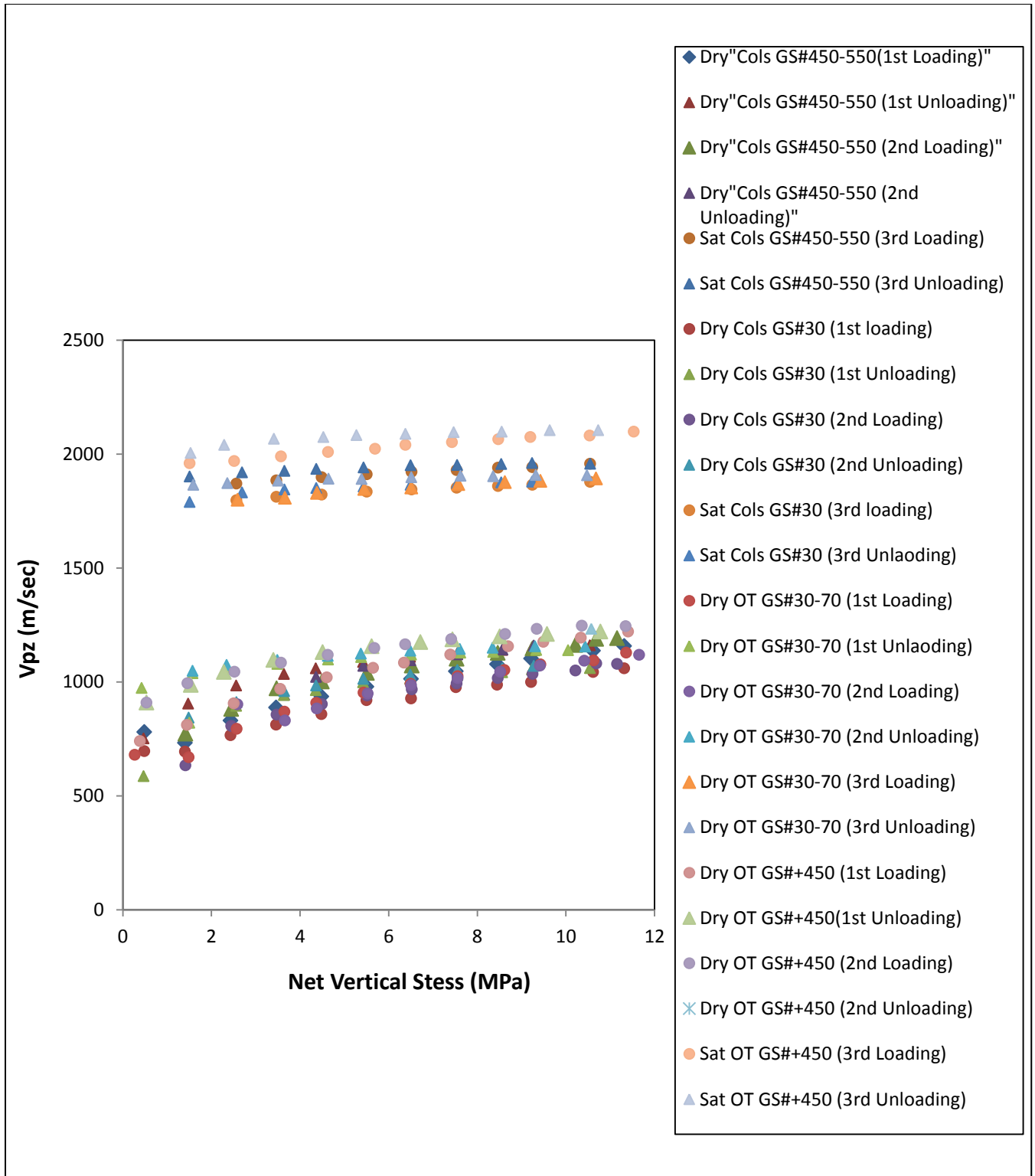
**Figure 4. 18 P-wave velocity plot against net vertical stress during loading and unloading cycles for all the dry and saturated samples with different grainsizes**

## 4.6. Dry and Saturated (Vsz) for all the samples during Loading & Unloading cycles:
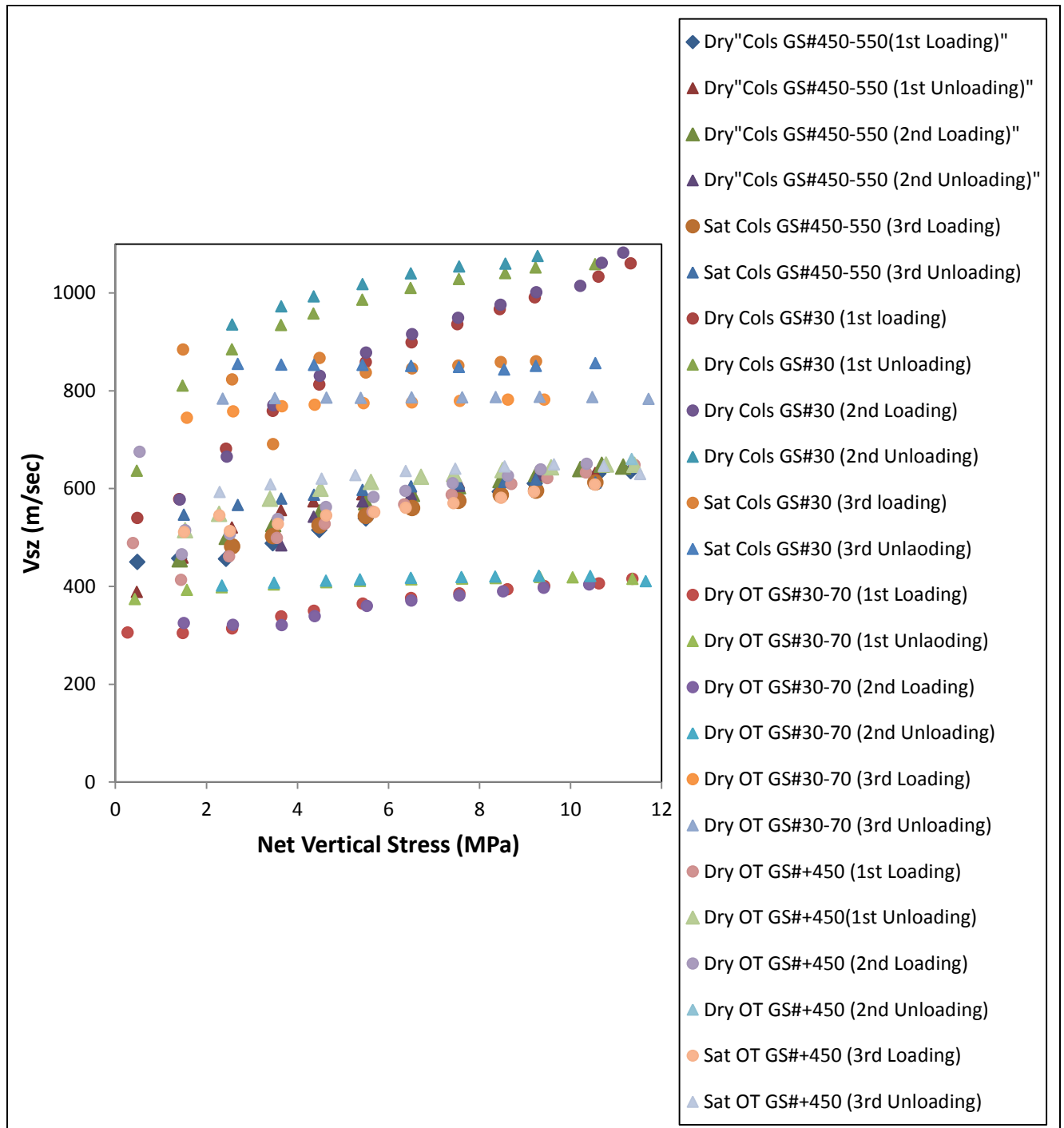


**Figure 4. 19 S-wave velocity plot against net vertical stress during loading and unloading cycles for all the dry and saturated samples with different grainsizes**

## 4.7. Dry and Saturated (Vp/Vs) for all the samples during Loading & Unloading cycles:

Vp-Vs relation is an important parameter to determine the lithology from seismic and sonic log and can be used for direct seismic interpretation for pore fluid using AVO analysis [20]. The vertical P wave velocity (Vpz) versus vertical S- wave velocity (Vsz) is plotted in figure 4.20 for all the samples dry and saturated with different grain sizes during loading and unloading cycles. The Vpz/Vsz is plotted against net vertical stress to illustrate the stress sensitivity. It was observed that at the higher stress level is at about 4.0 MPa Vpz/Vsz decreases relatively faster than the low stress level which is at about 2.5 MPa where Vpz/Vsz shows more or less stable trend. Parsad (2002) has also observed very high Vpz/Vsz value at low differential pressure and doesn't change so much above 2.0 MPa for water saturated sand. The Vpz/Vsz shows here for the dry sand is relatively less but stable as compared to the saturated where it just decreased rapidly and shows the different trend.

A Vpz/Vsz is widely used as a lithological indicator. However observation shows that it is difficult to distinguish by using only Vpz/Vsz ratio which decreases with increase in vertical stress as shown in figure 4.20. However by further evaluation of Vpz/Vsz along with the Vpz versus Vsz can be used as an indicator for the lithology.
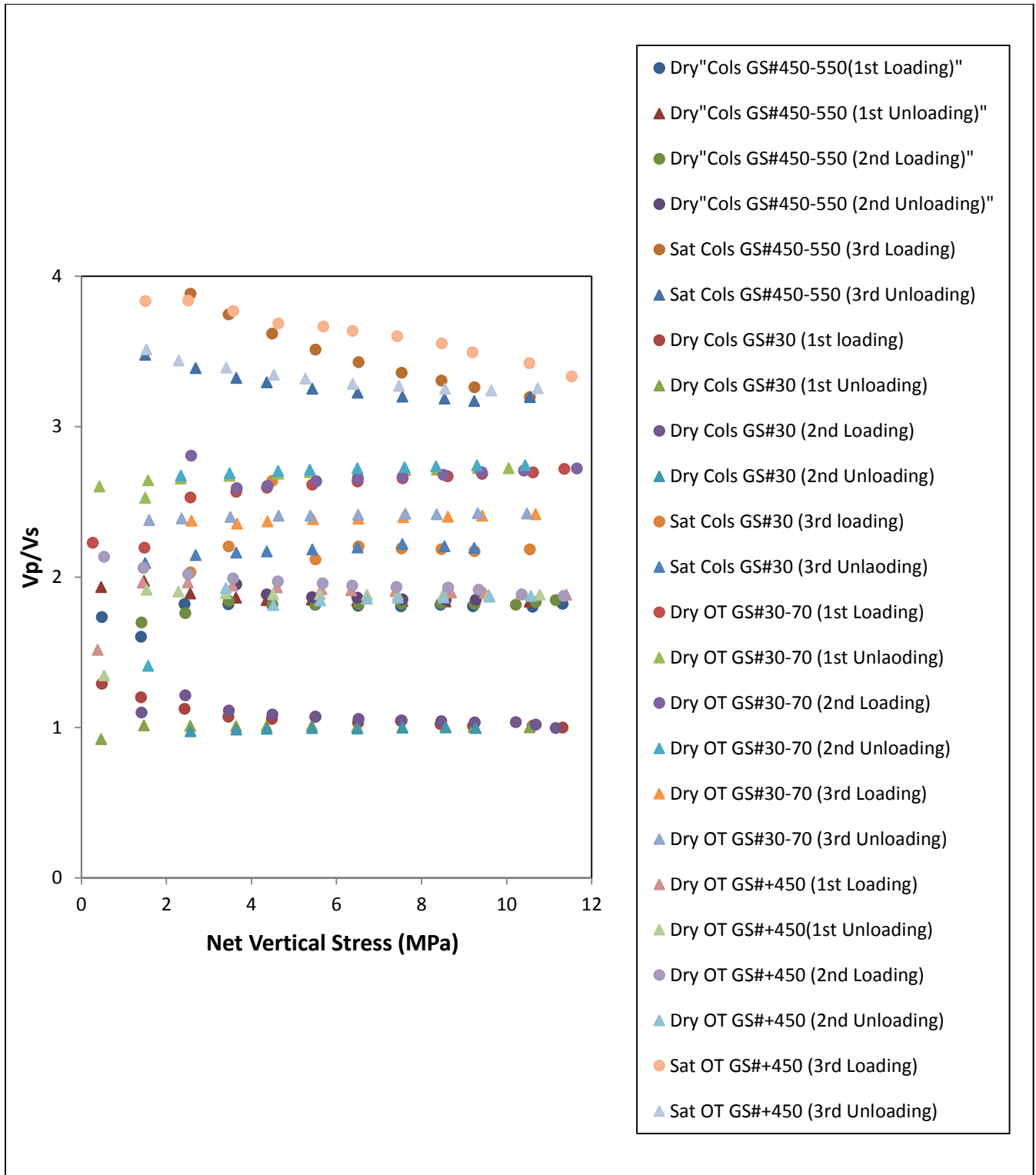
**Figure 4. 20 (Vp/Vs) velocity plot against net vertical stress during loading and unloading cycles for all the dry and saturated samples with different grainsizes**

## 4.8. Case#02

## 4.8.1. Effect of vertical Stress On vertical Strain:

The vertical stress are presented here as a function of the measured strain (mStrain= 1000*strain) for all the dry and saturated samples for both loading and unloading in figure 4.21. All the data presented here graphically shows the stress sensitivity until 1.5 MPa net vertical stresses. All the samples are showing less stress sensitivity as in the start of the loading but as the loading or stresses increases strain also increases which shows the strain sensitivity with stress. All the samples were compacted up to 11.0 MPa. OT (GS#30-70) shows comparatively high stress sensitivity as compared to the other samples. The factor which is most important to be observed is that all the samples more or less showing the inelastic behavior because none of the sample returns to its original shape which is strain hysteresis. It is also observed that all the samples are showing higher strain values at the highest stress level. However for all the samples friction of the piston and wall needs to be considered.
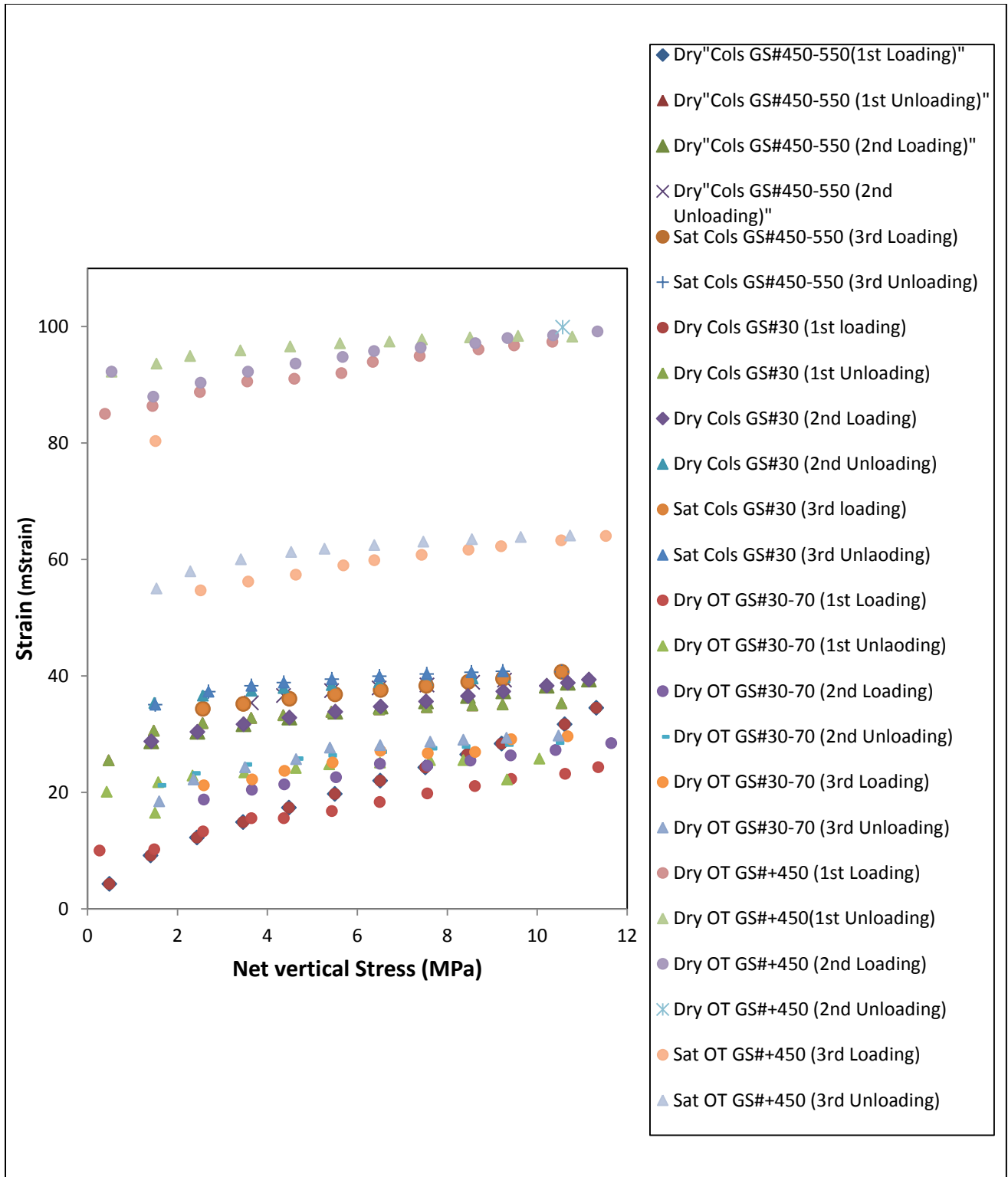
**Figure 4. 21 Strain plot against net vertical stress during loading and unloading cycles for all the dry and saturated samples with different grainsizes showing the strain sensitivity and strain hysteresis**

# 4.9.  Case#02:

## 4.9.1.    Effect of vertical stress on porosity:

The reduction on porosity is not only depends on the applied stresses but the other factors in porosity reduction are also need to be discussed and considered. The sediments subjected to mechanical compaction after deposition as it subjected to overburden pressure. The observation made here can be compare with only for shallow depths of the subsurface since the sediments are subjected to chemical and digenetic processes which are briefly discussed in chapter two section 2.2.1. The initial porosity for all the samples were measured with the help of a formula mentioned above in chapter three section 3.5. Figure 4.22 is showing the decrease in porosity with in an increase in net vertical stress. The purpose of showing this graph is to get an idea of porosity reduction with overburden stresses. However reduction on porosity seems to be more or less stable in all samples except for the few ones. It was observed that the change in porosity during loading and unloading cycles was very low as stress is not the only factor involved in porosity reduction as discussed above.
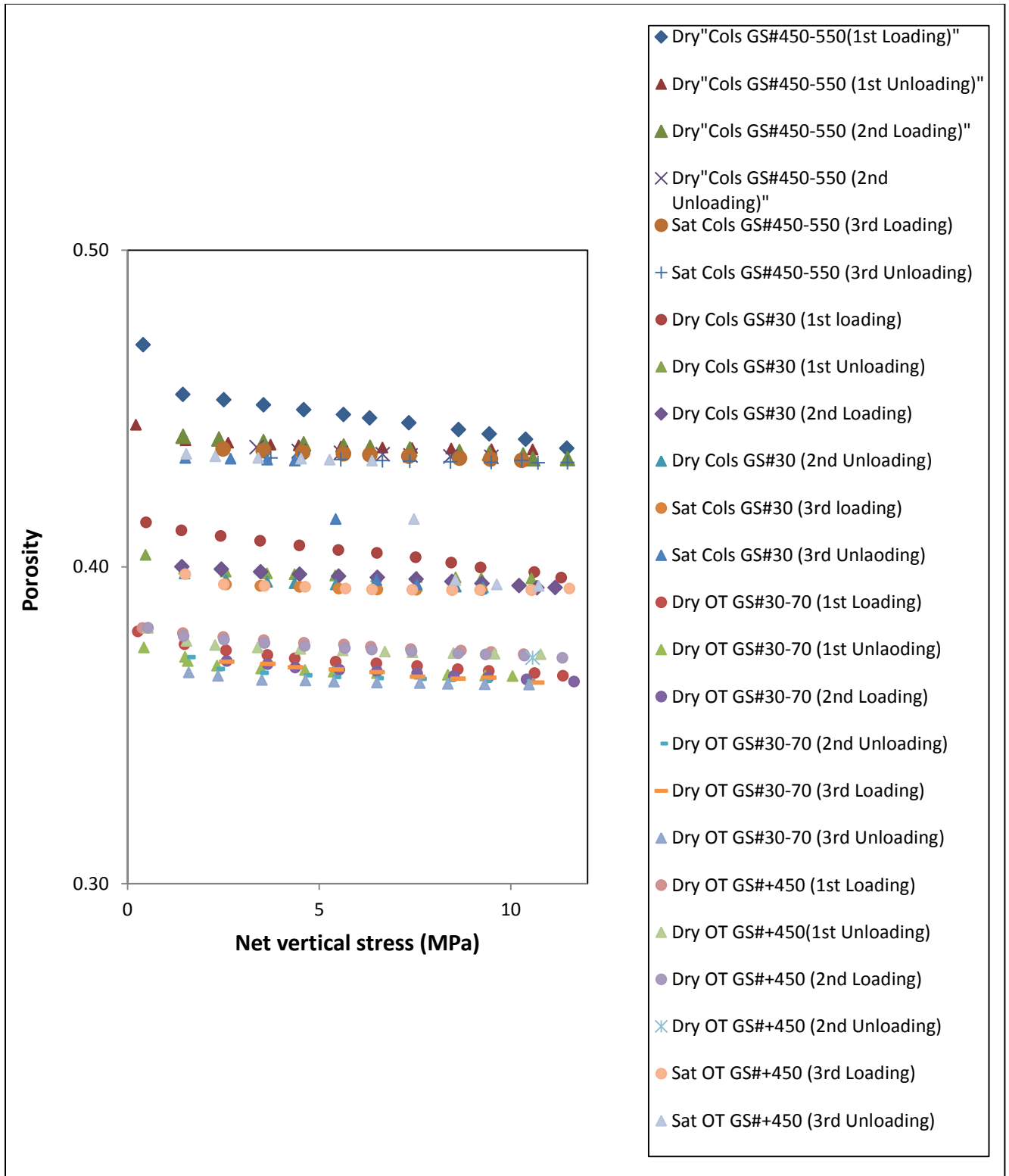
**Figure 4. 22 Porosity plot against net vertical stress during loading and unloading cycles for all the dry and saturated samples with different grainsizes showing the porosity change with stress**

# Chapter 5: Conclusion and Future Work

## 5.1. Conclusion:

To explore the acoustic and elastic properties of the unconsolidated sand in an oedometer setup in the laboratory, the effect on vertical stress on velocities, effect of fluid on velocities, effect of stress on strain and porosity were measured.

- The vertical P- and S- wave velocities measured in low concentration of brine are found much lower than the velocities measured with high concentration of brine which shows that the velocity has a direct relation with the concentration of the brine.
- Vpz and Vsz are found more stress sensitive in high percentage of brine and vice versa.
- Vpz measures in saturated sand are found much higher than the dry one.
- Vsz measures in both the dry and saturated case are found more or less same which shows that fluid has no effect on the S- wave velocity.
- Vp/Vs decreases with in an increase in net vertical stress, but it was observed that at higher stress level at about 4.0 MPa it decrease relatively faster than at low stress level. While at about 2.5 MPa it shows more or less stable trend.
- It was found that samples with high concentration of brine show high strain sensitivity as compared to samples with low concentration. Similarly in case of samples with different grain sizes strain sensitivity was found less during start of the loading while it got higher values as the net vertical stress increases. All the samples show inelastic behavior as none of the sample returns to their original shape which shows the strain hysteresis.
- Porosity reduction for all the samples both dry and saturated was found very low due to stress as it was only mechanical compaction due to an increase in net vertical stress.

## 5.2. Future Work:

In the present project, compressional and shear wave velocities were measured in an oedometer setup only in uniaxial strain condition but can be further evaluated by measuring in triaxial test setup with different boundary conditions which could provide the vertical and lateral strain measurements in combination with axial and radial P- and S- wave velocities which would give the comparison between both setups.

Although the main idea was to find the effect pore fluid on frame moduli but due to time constrain only velocities, porosity and strain sensitivity has been evaluated but this data can be further use for the evaluation of velocities behavior with pore pressure and different lithologies. As the velocities behavior in both dry and saturated case has been done in the present work so it can be further use to find the relationship between dry and saturated shear moduli for all the cases.

As the acoustic velocities are dependent on lithology, the present work is totally based on the one lithology which was sand but it can also be interesting to see the velocities effect in different lithologies like in clay or sand clay mixture with different contents of both lithologies. Similarly the present results can be further initiated for detail research like behavior of anisotropy with clay content, change in reflection coefficient with change in saturation of fluid etc.

# References:

[1] Biot, Maurice Anthony, and Ivan Tolstoy. Acoustics, elasticity, and thermodynamics of porous media: twenty-one papers. Acoustical Society of Amer, 1992

[2] Jaeger, John Conrad, Neville GW Cook, and Robert Zimmerman. Fundamentals of rock mechanics. Wiley. com, 2009

[3] Wang, Herbert F. Theory of Linear Poroelasticity: With Applications to Geomechanics and Hydrogeologoy.  Princeton University Press, 2000

[4] Biot, Maurice A. "General theory of three-dimensional consolidation." Journal of applied physics 12.2 (1941): 155-164

[5] Rutqvist, Jonny, and Ove Stephansson. "The role of hydromechanical coupling in fractured rock engineering." Hydrogeology Journal 11.1 (2003): 7-40

[6] Lectures notes by Stephen lippard (Petroleum Geology)

[7] Biot, Maurice A. "Mechanics of deformation and acoustic propagation in porous media." Journal of applied physics 33.4 (1962): 1482-1498.

[8] Walton, Otis R. "Numerical simulation of inelastic, frictional particle-particle interactions." Particulate two-phase flow 25 (1993): 884-911.

[9] Johnson, Kenneth L. "Contact mechanics." Cambridge University, Cambridge (1995).

[10] Walton, Otis R. "Numerical simulation of inelastic, frictional particle-particle interactions." Particulate two-phase flow 25 (1993): 884-911.

[11] Reservoir Seismic Lecture notes, by Rune M. Holt.

[12] Ojala, I. O., and E. Fjær. "The effective stress coefficient in porous sandstone." 1st Canada-US Rock Mechanics Symposium. American Rock Mechanics Association, 2007.

[13] Siggins, Anthony F., and David N. Dewhurst. "Saturation, pore pressure and effective stress from sandstone acoustic properties." Geophysical Research Letters 30.2 (2003).

[14-19] Pictures taken from the previously done project.

[20] Bachrach, Ran, and Per Avseth. "Rock physics modeling of unconsolidated sands: Accounting for nonuniform contacts and heterogeneous stress fields in the effective media approximation with applications to hydrocarbon exploration."*Geophysics* 73.6 (2008): E197-E209.
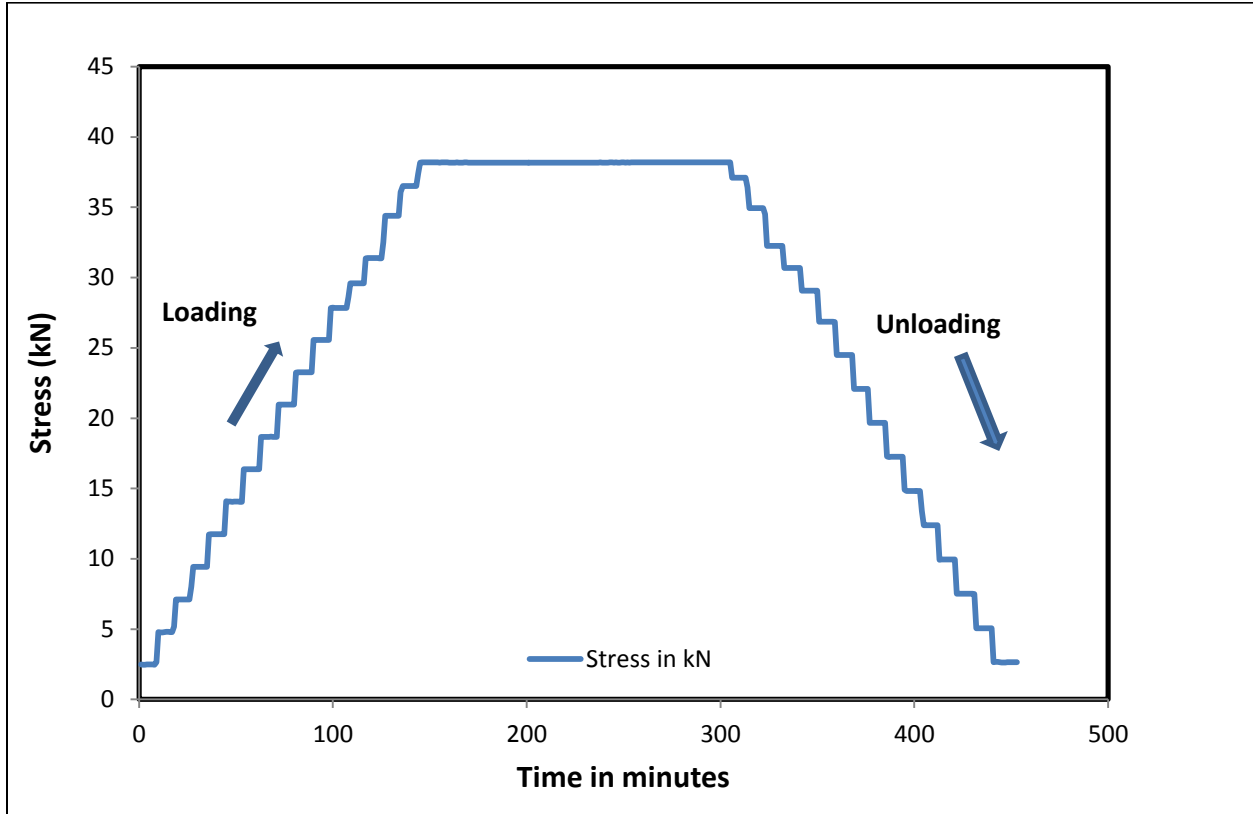
# Appendices

## Appendix A

**A.1. Test plans for case#01 (brine saturated Ottawa (OT) sand used in oedometer test system**
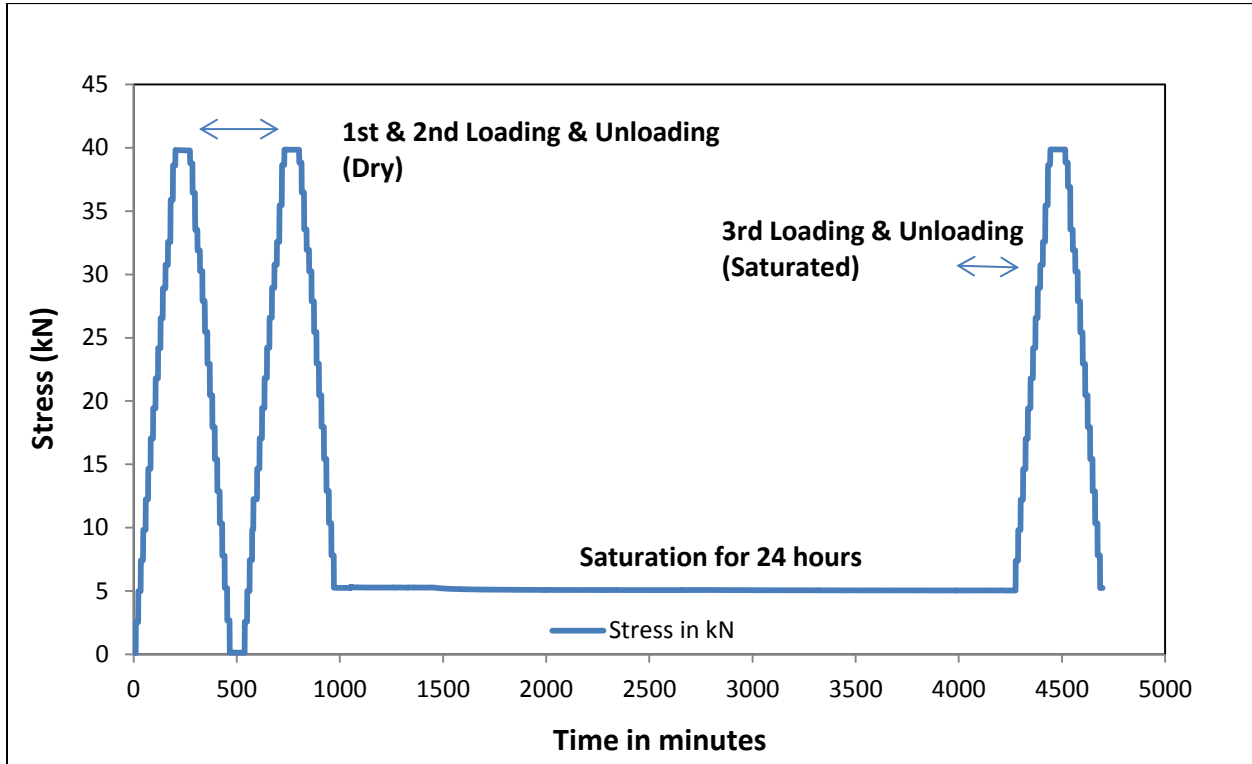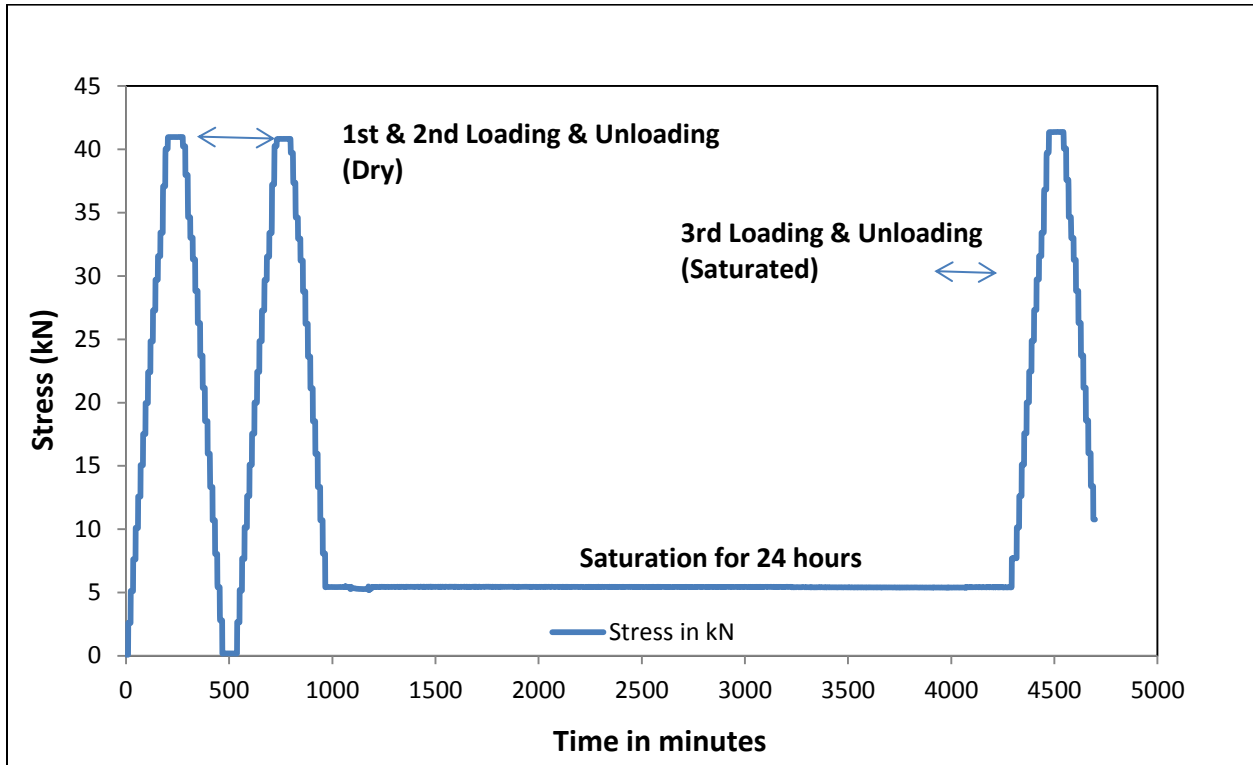
**OT (0 wt %):**
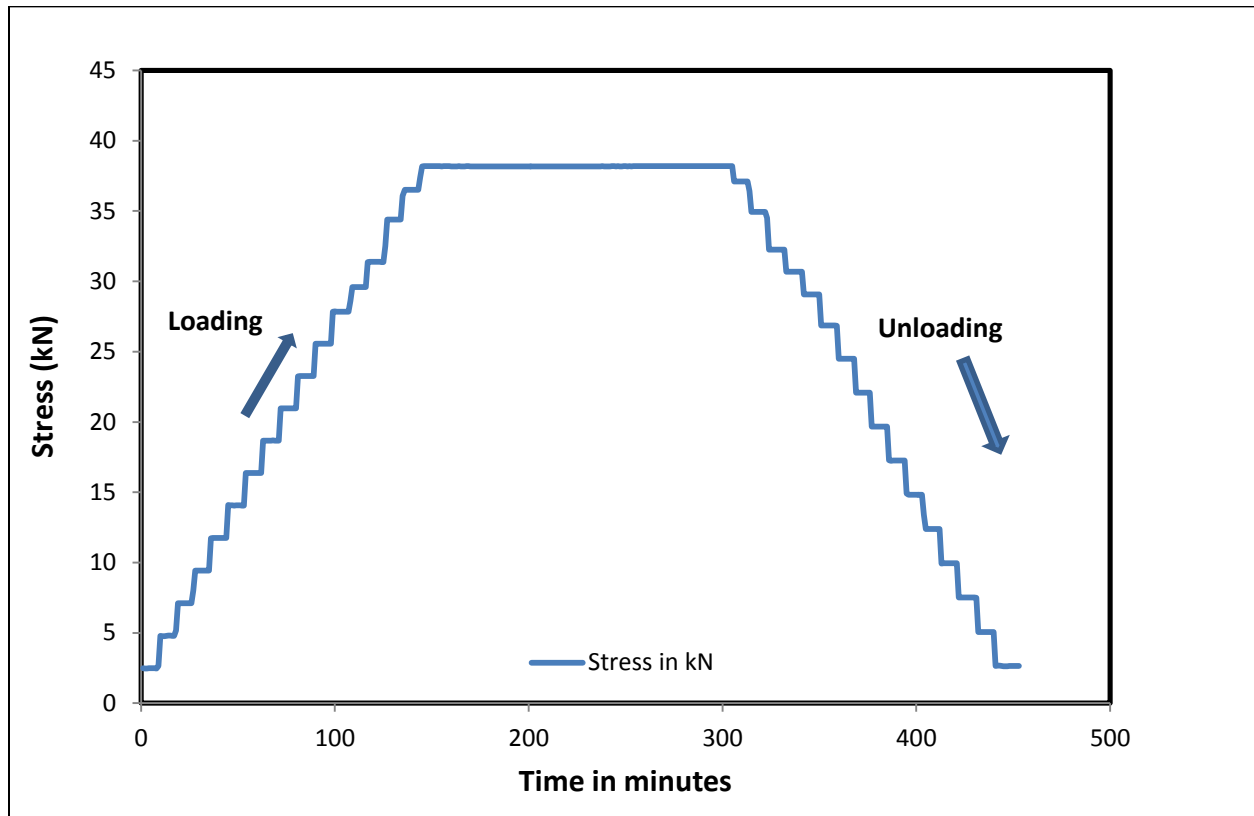
**OT (7 wt %):**

**A.2. Test Plan used for case #02 for all dry and saturated sand samples used in oedometer system**
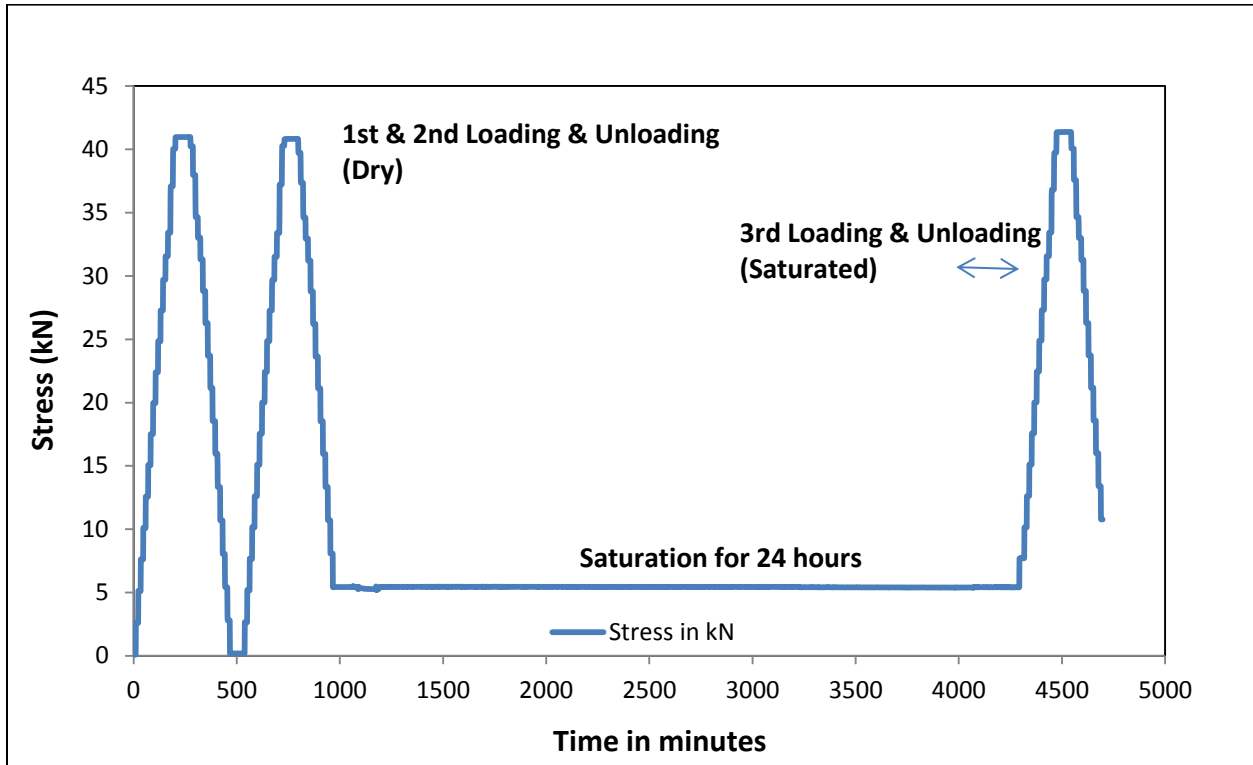
**Dry and saturated Columbia sand (GS#450-550):**

**Dry & Saturated Columbia Sand (GS#30):**

**Dry & Saturated Ottawa (OT) Sand (GS#30-70):**

# Appendix B:

## B.1. Experimental results for case#01 (Unloading):

Table B.1: experimental results for 0 wt % brine (Unloading)

| 0 wt % Unloading | | | | |
|---|---|---|---|---|
| Net Vertical Stress (Mpa) | Vpz (m/sec) | Vsz (m/sec) | Strain ( Av mStrain) | Porosity |
| 10.706 | 1171 | 683 | 38.31316465 | 0.42 |
| 10.244 | 1171 | 680 | 38.13714705 | 0.41 |
| 9.749 | 1171 | 677 | 37.77044371 | 0.41 |
| 9.237 | 1171 | 669 | 37.48231966 | 0.41 |
| 8.769 | 1171 | 669 | 37.03703704 | 0.41 |
| 8.200 | 1169 | 658 | 36.58629752 | 0.41 |
| 7.520 | 1172 | 657 | 35.52239282 | 0.41 |
| 6.821 | 1138 | 644 | 34.32043885 | 0.41 |
| 6.115 | 1134 | 644 | 33.07205721 | 0.41 |
| 5.407 | 1123 | 629 | 25.47335069 | 0.41 |
| 4.698 | 1110 | 624 | | 0.41 |
| 3.629 | 1083 | 605 | | |
| 2.916 | 1053 | 600 | | |
| 2.203 | 1012 | 578 | | |
| 1.845 | 967 | 579 | | |
| 1.131 | 888 | 596 | | |
| 0.774 | 766 | 603 | | |

Table B.2: experimental results for 3.5wt % brine (Unloading)

| 3.5 wt % Unloading | | | | |
|---|---|---|---|---|
| **Net Vertical Stress (Mpa)** | **Vpz (m/sec)** | **Vsz (m/sec)** | **Strain ( Av mStrain)** | **Porosity** |
| 10.706 | 2059 | 318 | 42.563 | 0.43 |
| 10.244 | 2057 | 317 | 42.639 | 0.43 |
| 9.749 | 2057 | 317 | 42.281 | 0.43 |
| 9.237 | 2054 | 316 | 41.901 | 0.43 |
| 8.769 | 2055 | 315 | 41.346 | 0.43 |
| 8.200 | 2051 | 314 | 40.712 | 0.43 |
| 7.520 | 2044 | 312 | 39.790 | 0.43 |
| 6.821 | 2043 | 310 | 38.794 | 0.43 |
| 6.115 | 2035 | 308 | 37.957 | 0.43 |
| 5.407 | 2030 | 304 | 35.955 | 0.43 |
| 4.698 | 2022 | 298 | 31.128 | 0.44 |
| 3.629 | 2018 | 295 | | |
| 2.916 | 2011 | 288 | | |
| 2.203 | 1998 | 276 | | |
| 1.845 | 1989 | 265 | | |
| 1.131 | 1965 | 255 | | |
| 0.774 | 1948 | 223 | | |

Table B.3: experimental results for 7wt % brine (Unloading)

| 7 wt % Unloading | | | | |
|---|---|---|---|---|
| Net Vertical Stress (Mpa) | Vpz (m/sec) | Vsz (m/sec) | Strain ( Av mStrain) | Porosity |
| 10.706 | 2423 | 697 | 29.63181 | 0.42 |
| 10.244 | 2415 | 691 | 29.26167 | 0.41 |
| 9.749 | 2413 | 687 | 28.75879 | 0.41 |
| 9.237 | 2402 | 683 | 28.25580 | 0.41 |
| 8.769 | 2393 | 677 | 27.68087 | 0.41 |
| 8.200 | 2382 | 669 | 26.91318 | 0.41 |
| 7.520 | 2358 | 661 | 25.94600 | 0.41 |
| 6.821 | 2328 | 651 | 24.64576 | 0.41 |
| 6.115 | 2307 | 638 | 22.63472 | 0.41 |
| 5.407 | 2297 | 623 | 18.26423 | 0.41 |
| 4.698 | | 603 | | 0.41 |
| 3.629 | | 577 | | |
| 2.916 | | 541 | | |
| 2.203 | | 481 | | |
| 1.845 | | 443 | | |
| 1.131 | | | | |
| 0.774 | | | | |